SA01

Fibroblast-Myocyte interactions and their impact on cardiac electrophysiology

Patrizia Camelliti[1]

[1]University of Surrey, Guildford, United Kingdom

The heart is a complex organ composed of multiple cell types working together to maintain its rhythmic and contractile function. Among the key cell types within the heart are myocytes and cardiac fibroblasts. Myocytes are the primary muscle cells responsible for the mechanical contraction of the heart, enabling it to pump blood efficiently throughout the body. Fibroblasts are the most abundant non-myocyte cells in the heart, and they are responsible for producing and maintaining the extracellular matrix, which provides structural and mechanical support for the cardiac tissue. Fibroblasts number further increases with ageing and pathological conditions [1]. Traditionally considered as passive cells providing structural support, research has now unveiled an active and dynamic role for cardiac fibroblasts in modulating cardiac electrophysiology. In addition to forming passive obstacles to electrical conduction, fibroblasts have been proposed to actively affect cardiac conduction, myocyte excitability, contractility, action potential duration and calcium cycling. Mechanisms include heterocellular cell-cell coupling and paracrine communication [2]. Functional fibroblast-myocyte coupling mediated by gap junctions or tunnelling nanotubes has been observed both *in vitro* and *in situ* in animal models [3,4,5]. Importantly, *in situ* this coupling is limited to cells in the sinoatrial node and in the ventricle at the border zone of post-myocardial infarcts [5,6]. Coupling also occurs between senescence fibroblasts and myocytes at the infarct border zone in the aged rabbit heart, promoting significant arrhythmogenic remodelling [7]. Paracrine communication, mediated by cytokines and growth factors released by cardiac fibroblasts, has also been shown to influence myocyte electrophysiology and calcium handling in animal cell cultures [8,9]. Recently, advanced human cell coculture systems mimicking different cell-cell interaction modalities have been employed to assess the contribution of contact *versus* paracrine interactions. Activated human cardiac fibroblasts exert adverse effects on the electrophysiological and Ca^{2+} handling of human myocytes and downregulate voltage channels ($K_V4.3$, $K_V11.1$ and Kir6.2) and SERCA2a calcium pump. Interleukin-6 and connexin43 were identified as paracrine- and contact-mediators driving these effects [10]. Thus, fibroblast-myocyte interactions are complex and dynamic processes that play a crucial role in cardiac electrophysiology. Understanding these interactions can help to elucidate the mechanisms of normal and abnormal cardiac function, as well as to develop novel strategies for preventing and treating cardiac arrhythmias and progression to heart failure. Details of fibroblast-myocyte interactions in disease conditions such as ischemia-reperfusion injury, hypertrophic and dilated cardiomyopathy as well as in the ageing heart are still poorly explored and form a potentially exciting target for further research. Emerging tools and experimental model systems [11,12] will be invaluable to accelerate this research.

[1] Johnson RD & Camelliti P. Role of non-myocyte gap junctions and connexin hemichannels in cardiovascular health and disease: novel therapeutic targets? Int J Mol Sci. 2018 Mar 15;19(3):866. [2] Pellman J, Zhang J, Sheikh F. Myocyte-fibroblast communication in cardiac fibrosis and srrhythmias: mechanisms and model systems. J Mol Cell Cardiol. 2016 May; 94: 22–31. [3] Vasquez, C. et al. Enhanced fibroblast–myocyte interactions in response to cardiac injury. Circ Res. 2010; 107: 1011-1020. [4] Quinn, T. A. et al. Electrotonic coupling of excitable and nonexcitable cells in the heart revealed by optogenetics. Proc Natl Acad Sci USA 113,

14852 (2016). [5] Mahoney, V. M. et al. Connexin43 contributes to electrotonic conduction across scar tissue in the intact heart. Sci Rep. 2016; 6, 26744. [6] Camelliti, P., Green Colin, R., LeGrice, I. & Kohl, P. Fibroblast Network in Rabbit Sinoatrial Node. Circ Res. 2004; 94: 828-835. [7] Baggett BC, Murphy KR, Sengun E, Mi E, Cao Y, Turan NN, Lu Y, Schofield L, Kim TY, Kabakov AY, Bronk P, Qu Z, Camelliti P, Dubielecka P, Terentyev D, del Monte F, Choi B-R, Sedivy J, Koren G. Myofibroblast senescence promotes arrhythmogenic remodeling in the aged infarcted rabbit heart. Elife. 2023 May 19;12:e84088. doi: 10.7554/eLife.84088. [8] Pedrotty DM, Klinger RY, Kirkton RD, Bursac N. Cardiac fibroblast paracrine factors alter impulse conduction and ion channel expression of neonatal rat cardiomyocytes. Cardiovasc Res. 2009; 83: 688-697. [9] Cartledge, J. E. et al. Functional crosstalk between cardiac fibroblasts and adult cardiomyocytes by soluble mediators. Cardiovasc Res. 2015; 105: 260-270. [10] Johnson RD, Mcvey JH, Camelliti P. Human myofibroblasts increase the arrhythmogenic potential of human-induced pluripotent stem cell-derived cardiomyocytes. Cardiovascular drugs and therapy 34 (2), 280-281. [11] Wu Q, Ross AJ, Ipek T, Thompson GH, Johnson RD, Wu C, Camelliti P. Hydroxychloroquine and azithromycin alter the contractility of living porcine heart slices. Front Pharmacol. 2023; 202314: 1127388. [12] Cox-Pridmore DM, Castro FA, Silva SRP, Camelliti P, Zhao Y. Emerging bioelectronic strategies for cardiovascular tissue engineering and implantation. Small. 2022; 18 (17), 2105281.

SA02

Cardiac fibroblast activation and reversal and their interaction with cardiomyocytes

Caitlin Hall[1], Jonathan Law[1], Max Cumberland[1], Jasmeet S Reyat[1], Christopher Weston[1], Chrisopher O'Shea[1], Katja Gehmlich[1], Chris Denning[2], Davor Pavlovic[1]

[1]University of Birmingham, Birmingham, United Kingdom, [2]University of Nottingham, Nottingham, United Kingdom

Introduction: Cardiac fibroblasts (cFbs) maintain the extracellular matrix and provide a scaffold for cardiomyocytes (CMs). Following injury, cFbs become activated to myofibroblasts (MyoFbs) to aid in wound healing and repair. In disease, myofibroblasts contribute to pathological remodelling and cardiac fibrosis. This study aimed to investigate the potential for reversal of chronically activated human cardiac fibroblasts in 2D culture. We also evaluated the effects of quiescent and activated human cardiac fibroblasts on cardiomyocyte electrical and contractile function.

Methods: Primary human cFbs and human induced pluripotent stem cell derived cFbs (hiPSC-cFbs) were assessed for activation following 2-4 weeks of culture on stiff culture plastic (E = ~ 3 GPa) and in the presence of 10 ng/ml TGF-β. Myofibroblast reversal was assessed using TGF-β receptor inhibition (10 μM SB431542). mRNA and protein expression of activation markers α-SMA, collagens 1 and 3 were investigated. α-SMA expression was also assessed using immunofluorescence staining. Quiescent or activated iPSC-cFbs were plated on top of iPSC-CMs for 5 days. Contraction was assessed using MUSCLEMOTION and electrical activity using optical mapping.

Results: Primary cFbs and hiPSC-cFbs activate to myofibroblasts following culture on stiff plastic. In the absence of any chemical stimuli. Long term culture on stiff plastic led to both cell types becoming unresponsive to TGF-β stimulation or TGF-β receptor inhibition. hiPSC-cFbs remained quiescent in the presence of SB431542, while still being able to activate into MyoFbs upon TGF-β exposure (evident through increased α-SMA and collagen 1). Co-culture for five days with either cFb type did not affect CM contraction or calcium transients. TGF-β-exposed CMs showed increased action potential duration 50, 70 and 90 compared to SB431542-treated CMs, but no significant changes occurred with quiescent or activated fibroblasts.

Conclusions: Human cFbs activate independently of any external stimulus during standard 2D culture. Chronically activated human cFbs have a limited **potential for reversal to a quiescent phenotype.** Activation status of hiPSC-cFbs does not significantly affect contraction or electrical handling of iPSC-CMs.

SA03

Exploring the role of neuronal dysfunction in inherited arrhythmia syndromes

Molly O'Reilly[1], Fern Bosada-Musselwhite[1], Tanja de Waal[1], Marieke Veldkamp[1], Simona Casini[1], Carol Ann Remme[1]

[1]Experimental Cardiology, Amsterdam UMC location AMC, Amsterdam, The Netherlands, Amsterdam, Netherlands

Background: Inherited arrhythmia syndromes are a leading cause of sudden cardiac death in young and otherwise healthy patients. These are often caused by mutations in genes that encode ion channels or transporters, leading to conditions such as Brugada Syndrome (BrS), Long QT Type 3 (LQT3), and Catecholaminergic Polymorphic Ventricular Tachycardia (CPVT).

BrS and LQT3 are associated with mutations in *SCN5A* (encoding sodium channel, $Na_v1.5$), whilst CPVT is caused by mutations in *RYR2* (encoding ryanodine receptor 2, RyR2). Investigation into the effects of these mutations have exclusively been performed in cardiac cells. However, these ion channels are also present in neuronal tissue, including intracardiac neurons[1] (which modulate cardiac function). Moreover, patients often present with clinical signs of dysfunction of the autonomic nervous system.

Aim: Our novel research line aims to investigate the neuronal phenotype induced by these ion channel mutations, using arrhythmia mouse models to assess functional alterations as well as broader autonomic remodelling. Ultimately, we will assess the contribution of this to arrhythmogenesis.

Results: Using immunohistochemistry approaches, we reveal for the first time that both $Na_v1.5$ and RyR2 are also expressed in mouse stellate ganglia (a crucial autonomic modulator of cardiac function). Current functional investigations, including patch clamp analysis, are aimed at assessing the functional consequences of *Scn5a* and *RyR2* mutations in stellate and intracardiac ganglia in mouse models of BrS, LQT3 and CPVT. These experiments also allow for investigation of the modulatory effects of pharmacological interventions. In addition, autonomic remodelling in stellate/intracardiac ganglia and (ventricular) myocardium is currently being assessed through RNA sequencing, immunohistochemistry in mouse heart cryosections, and whole-heart neuronal imaging. Findings from these investigations will be presented.

Conclusions: All neurons that modulate heart function (stellate ganglion and intracardiac neurons) express $Na_v1.5$ and RYR2. Mouse models of BrS/LQTS/CPVT are employed to investigate the consequences of *Scn5a*/*RyR2* mutations on neuronal (dys)function and their potential role in arrhythmogenesis.

1 Scornik, F. S., et al., (2006). Functional expression of "cardiac-type" Nav1.5 sodium channel in canine intracardiac ganglia. Heart rhythm, 3(7), 842–850.

SA04

Towards new therapeutics in atrial fibrillation.

svetlana reilly[1], Lucia Moreira[1,2]

[1]University of Oxford, Oxford, United Kingdom, [2]University of Oxford, Oxford, United Kingdom

Atrial fibrillation, the most common cardiac arrhythmia, is an important contributor to mortality and morbidity, and particularly to the risk of stroke in humans. Atrial-tissue fibrosis is a central pathophysiological feature of atrial fibrillation that also hampers its treatment; the underlying molecular mechanisms are poorly understood and warrant investigation given the inadequacy of present therapies. Here we show that calcitonin, a hormone product of the thyroid gland involved in bone metabolism, is also produced by atrial cardiomyocytes in substantial quantities and acts as a paracrine signal that affects neighbouring collagen-producing fibroblasts to control their proliferation and secretion of extracellular matrix proteins. Global disruption of calcitonin receptor signalling in mice causes atrial fibrosis and increases susceptibility to atrial fibrillation. In mice in which liver kinase B1 is knocked down specifically in the atria, atrial-specific knockdown of calcitonin promotes atrial fibrosis and increases and prolongs spontaneous episodes of atrial fibrillation, whereas atrial-specific overexpression of calcitonin prevents both atrial fibrosis and fibrillation. Human patients with persistent atrial fibrillation show sixfold lower levels of myocardial calcitonin compared to control individuals with normal heart rhythm, with loss of calcitonin receptors in the fibroblast membrane. Although transcriptome analysis of human atrial fibroblasts reveals little change after exposure to calcitonin, proteomic analysis shows extensive alterations in extracellular matrix proteins and pathways related to fibrogenesis, infection and immune responses, and transcriptional regulation. Strategies to restore disrupted myocardial calcitonin signalling thus may offer therapeutic avenues for patients with atrial fibrillation.

SA05

Physiological Heterocellular Interactions in vitro: Living Myocardial Slices and Micro Vascularised Human Engineered Cardiac Tissue

Cesare Terracciano[1]

[1]National Heart &Lung Institute, Imperial College London, London, United Kingdom

Tissue and cellular adaptability and plasticity determine cardiac phenotypes but are difficult to elicit in in vitro models. In this talk, I will present two models where plasticity is accounted for: the living myocardial slices, subjected to electromechanical stimulation (Watson *et al.*, 2017, 2019; Pitoulis *et al.*, 2021), and the micro vascularised engineered myocardium, composed of human iPSC-derived cardiomyocytes and human microvascular endothelial cells (King *et al.*, 2022).

The living myocardial slices are the gold standard to study heterocellular interactions in vitro because they are derived from the whole, native myocardium, containing all the cellular and extracellular components. They can be obtained from hearts of many species, including human failing and non-failing hearts, can be cultured for several days/weeks and respond promptly to environmental changes. We have developed bioreactors to maintain and manipulate the electromechanical status of the slices in physiology and disease. We can specifically manipulate preload and/or afterload in long term cultures and have described methods to study individual cell types within the slices, or after isolation. We are thus able to simulate disease in slices, e.g. mechanical overload (Nunez-Toldra *et al.*, 2022), ischemia-reperfusion injury and focal injury. We can genetically modify living myocardial slices using viral vectors, opening novel and more relevant avenues for investigating cardiac disease.

The micro vascularised, IPSC-derived myocardium allows studying specifically into the cross talk between endothelial cells and cardiomyocytes when both contraction and vascular flow are present. In this model, contractility and flow in the engineered micro vessels can be manipulated and the consequences on the heterocellular interactions studied. This model is a step forward in physiological cardiac tissue engineering and represents a relevant tool to understanding cell-cell interaction in the heart.

King O, Cruz-Moreira D, Kermani F, Kit-anan W, Wang BX, Sunyosvszki I, Downing B, Fourre' J, Hachim D, Randi AM, Stevens MM, Rasponi M & Terracciano CM (2022). Functional microvascularisation of human myocardium in vitro. Cell Reports Methods. Nunez-Toldra R, Kirwin T, Ferraro E, Pitoulis FG, Nicastro L, Bardi I, Kit-Anan W, Gorelik J, Simon AR & Terracciano CM (2022). Mechanosensitive molecular mechanisms of myocardial fibrosis in living myocardial slices. ESC Hear Fail 9, 1400–1412. Pitoulis FG, Nunez-Toldra R, Xiao K, Kit-Anan W, Mitzka S, Jabbour RJ, Harding SE, Perbellini F, Thum T, de Tombe PP & Terracciano CM (2021). Remodelling of adult cardiac tissue subjected to physiological and pathological mechanical load in vitro. Cardiovasc Res; DOI: 10.1093/cvr/cvab084. Watson SA, Duff J, Bardi I, Zabielska M, Atanur SS, Jabbour RJ, Simon A, Tomas A, Smolenski RT, Harding SE, Perbellini F & Terracciano CM (2019). Biomimetic electromechanical stimulation to maintain adult myocardial slices in vitro. Nat Commun; DOI: 10.1038/s41467-019-10175-3. Watson SA,

Scigliano M, Bardi I, Ascione R, Terracciano CM & Perbellini F (2017). Preparation of viable adult ventricular myocardial slices from large and small mammals. Nat Protoc; DOI: 10.1038/nprot.2017.139.

SA06

Multi-scale modelling of cardiac heterogeneity from nanodomain to the whole heart

Michael Colman[1]

[1]*University of Leeds, Leeds, United Kingdom*

Heterogeneity and variability are important determinants of both normal and abnormal function of the heart. Cardiac cells and tissues exhibit heterogeneities and variability across a substantial range of spatial scales, from single dyads (nm) through whole cells (μm) to the whole-heart (mm-cm). Investigation of the interacting mechanisms by which these multi-scale heterogeneities ultimately lead to cardiac dysfunction is a major research challenge which cannot be met through traditional experimental techniques; novel joint computational-experimental approaches need to be developed to achieve this goal.

This talk will discuss a range of computational approaches to study heterogeneous structure-function relationships across the relevant spatial scales, from models of the single-nanodomain, through detailed models of individual cells, to models of the whole-heart. In particular, we will discuss modelling the mechanisms by which dysfunction of the intracellular calcium handling system is involved in the generation and sustenance of arrhythmia, and image-analysis approaches that facilitate integration between simulation and experiment. We will reveal novel mechanisms by which heterogeneity in the distribution of sub-cellular calcium handling channels can lead to mechanical dysfunction, the mechanisms by which independent cellular spontaneous activity synchronises into a focal excitation, and the interaction between these focal excitations and fibrosis which lead to complex trigger and substrate dynamics.

SA07

From microscale origin to whole heart manifestation: the journey of spontaneous Ca2+ release

Eef Dries[1]

[1]KU Leuven, Leuven, Belgium

Spontaneous Ca^{2+} release (SCR) events can cause triggered activities and initiate arrhythmias during disease remodeling. SCR events are traditionally studied by single cell or whole heart electrophysiology, but these techniques alone are limited in providing in-depth insights into complex cell-cell interactions and tissue microarchitecture. In our laboratory, a collection of data ranging from single cell level, multicellular tissue preparations up to in vivo animal models have shaped our current view as how SCR can contribute to arrythmia initiation. We have studied spontaneous loss of sarcoplasmic reticulum Ca^{2+} through ryanodine receptors (RyRs) at the subcellular level and found hyperactive RyRs being located in a microdomain outside the dyadic cleft in diseased myocytes. Single cell studies paired with in vivo observations from a large animal model with myocardial infarction suggested that these hyperactive RyRs can generate a substrate for arrhythmia and are a local initiator of triggered activities in the peri-infarct region. Also, work in multicellular tissue preparations showed a significant increase of SCR events and their propagation in living cardiac tissue slices from human heart failure patients. Collectively, complementary tools are used to dissect arrhythmia at the different multitude from aberrant SR Ca^{2+} release at the single cardiac myocyte level to the manifestation at the whole heart.

SA08

Cellular cross-talks in the aging heart

Julian Wagner[1], Lukas Tombor[1], Pedro Filipe Malacarne[2], Nivethitha Manickam[1], Katja Schmitz[1], Ariane Fischer[1], Marion Muhly-Reinholz[1], Wesley Abplanalp[1], David John[1], Sarajo Mohanta[3], Christian Weber[3], Andreas Habenicht[3], Stephan Angendohr[4], Ehsan Amin[5], Katharina Scherschel[6], Christian Meyer[6], Nikolaj Klöcker[5], Stefan Guenther[7], Thomas Boettger[7], Thomas Braun[7], Christian Bär[8], Minh-Duc Pham[1], Jaya Krishnan[1], Susanne Hille[9], Oliver Müller[9], Tarik Bozoglu[10], Christian Kupatt[10], Eleonora Nardini[11], Selma Osmanagic-Myers[11], Andreas Zeiher[12], Ralf Brandes[2], Guillermo Luxan[1], Stefanie Dimmeler[1]

[1]Institute of Cardiovascular Regeneration, Centre for Molecular Medicine, Goethe University Frankfurt, Theodor Stern Kai 7, 60590 Frankfurt, Germany., Frankfurt, Germany, [2]Institute for Cardiovascular Physiology, Goethe University Frankfurt, Theodor Stern Kai 7, 60590 Frankfurt, Germany., Frankfurt, Germany, [3]Institute for Cardiovascular Prevention, Ludwig-Maximilians-Universität München (LMU), 80336 Munich, Germany, Munich, Germany, [4]Department of Cardiology, Pulmonology and Vascular Medicine, Medical Faculty, Heinrich-Heine-University Düsseldorf, Moorenstraße 5, 40225 Düsseldorf, Germany., Düsseldorf, Germany, [5]Institute of Neural and Sensory Physiology, Medical Faculty and University Hospital Düsseldorf, Heinrich-Heine-University Düsseldorf, 40225 Düsseldorf, Germany., Düsseldorf, Germany, [6]Division of Cardiology/Angiology/Intensive Care, EVK Düsseldorf, cNEP, cardiac Neuro- and Electrophysiology Research Consortium, 40217 Düsseldorf, Germany., Düsseldorf, Germany, [7]Max Planck Institute for Heart and Lung Research, 61231 Bad Nauheim, Germany., Bad Nauheim, Germany, [8]Institute of Molecular and Translational Therapeutic Strategies (IMTTS), Hannover Medical School, Carl-Neuberg-Str. 1, 30625 Hannover, Germany., Hannover, Germany, [9]Department of Internal Medicine III, University Hospital Schleswig-Holstein, University of Kiel, Arnold-Heller-Strasse 3, 24105 Kiel, Germany., Kiel, Germany, [10]Klinik und Poliklinik für Innere Medizin I, University Clinic rechts der Isar, Technical University of Munich, Ismaninger Strasse 22, 81675 Munich, Germany., Munich, Germany, [11]Institute of Medical Chemistry, Center for Pathobiochemistry and Genetics, Medical University of Vienna, Vienna A-1090, Austria., Vienna, Austria, [12]German Center for Cardiovascular Research (DZHK), Partner Site Rhein-Main, 60590 Frankfurt, Germany., Frankfurt, Germany

Introduction: Aging is a major risk factor for impaired cardiovascular function. The aging heart is characterized by vascular dysfunction, increased hypertrophy, fibrosis and electrophysiological alterations. Studies show impaired endothelial cell function associates with senescence in aging. Since vessels are aligned with nerves, and this interplay is critical for tissue homeostasis, we investigated whether an impairment of the neuro-vascular interface may contribute to age-associated pathologies in the heart.

Methods and Results: To investigate the innervation of the aging mouse heart, we histologically assessed the cardiac autonomic nervous system in 12-week and 20-month old mice using the pan-neuronal marker Tuj1 and the sympathetic marker tyrosine hydroxylase. Interestingly, sympathetic innervation of the left ventricle, especially around arteries, was reduced by 0.66±0.07-fold with aging (n=9; $p<0.05$) indicating that aging reduces innervation of the left ventricle. Similar findings were observed in premature aging models of TERT-deficient and endothelial-transgenic progeria mice. Electrophysiological studies confirmed an increased incidence of ventricular arrhythmias and reduced heart rate variability in aged mice.

In order to determine the potential contribution of the neurovascular cellular cross-talk to the reduced innervation, we analyzed gene expression of isolated endothelial cells in the aging mouse heart by bulk RNA sequencing. Aging significantly induced the expression of genes associated with GO-terms related to neuronal cell death and axon injury. *Sema3a*, a known axon repelling factor, was significantly increased by 1.5±0.2-fold in endothelial cells of aged mice hearts, a finding which was confirmed by qPCR and by histology at protein level ($p<0.05$). Next we determined the mechanism of *Sema3a* de-repression. We show that miR-145 acts as an up-stream regulator of *Sema3a* expression. miR-145-/- mice showed increased Sema3a expression and reduced cardiac innervation.

We observed an increase in acidic β-galactosidase activity as a marker for cellular senescence in the aging heart, particularly in the proximate arterial space. In addition, *Sema3a* expression was significantly increased in senescent endothelial cells *in vitro*, thus suggesting a putative role for senescence to impair cardiac innervation. To test whether eliminating senescent cells may restore left ventricular axon density, we treated 18-month old mice with a combination of the two senolytic drugs dasatinib and quercetin, which are known to deplete senescent cells *in vivo*. After 2 months of senolytic treatment, cellular senescence was reduced by 0.4±0.1-fold ($p<0.05$) in the aging heart in parallel with reduced expression of endothelial *Sema3a.* Importantly, senolytic treatment restored ventricular innervation (by 1.8±0.4-fold vs. old-placebo mice), augmented heart rate variability, and normalized electrophysiological abnormalities (all $p<0.05$).

Conclusion: In conclusion, we show that aging augments axon repelling signals in endothelial cells and reduces left ventricular innervation. The depletion of senescent cells prevented age-induced impairment of innervation and normalized electrophysiological abnormalities suggesting a critical role of senescence-associated axon repulsion in the aging heart.

SA09

Signalling between cardiomyocyte InsP3Rs and RyRs elicits arrhythmogenic activity in human heart failure.

Llewelyn Roderick[1]

[1]KULeuven, Leuven, Belgium

Heart failure (HF) is a leading cause of cardiovascular mortality and morbidity. While pump failure is a frequent cause of mortality, up to 50% of deaths are due to sudden cardiac death following lethal arrhythmias. Dysregulation in Ca^{2+} handling has emerged as a key mediator of these arrhythmias. The rhythmic contraction of cardiomyocytes necessary for the efficient pumping of the heart is mediated by the process of excitation contraction coupling (EC) whereby Ca^{2+} entering the cell via L-type Ca^{2+} channels during the action potential activates Ca^{2+} release through Ryanodine Receptor channels (RyR) on the Sarcoplasmic Reticulum (SR) Ca^{2+} store, which then engages the contractile machinery to induce cell contraction. This mechanism is highly dependent upon the synchronized release of Ca^{2+} from clusters of RyRs dispersed throughout the cytosol, predominantly at the Z lines. Ensuring the coupling of Ca^{2+} entry and SR Ca^{2+} release are T-tubular invaginations of the sarcolemma that bring its voltage gated channels into close proximity with RyRs on the SR at cell compartments termed dyads. During heart failure, T-tubules are lost leading to reduced coupling between L-type channels and RyRs, which in turn reduces Ca^{2+} release synchrony as well as increasing arrhythmogenic Ca^{2+} waves. We have identified increased expression of a second SR Ca^{2+} channel, the $InsP_3$ receptor ($InsP_3R$), in animal models of CV disease and in human heart failure. This channel is engaged by $InsP_3$ generated downstream of G-protein coupled receptors such as those liganded by the neurohormones endothelin-1 and Angiotensin, which are also elevated in disease. We find potent effects of $InsP_3$ on Ca^{2+} handling in voltage clamped cardiomyocytes isolated from failing human hearts in comparison to cardiomyocytes from age-matched non failing hearts. Specifically, in the presence of $InsP_3$, Ca^{2+} transient amplitude was reduced and frequency of elementary Ca^{2+} release events (Ca^{2+} sparks) via RyRs was increased. RyRs were required for the action of $InsP_3$, suggesting Ca^{2+} channel crosstalk, an observation that was supported by super resolution microscopy. The effects of $InsP_3$ were most prominent at RyRs that were not coupled to the T-tubular membrane at dyads. Mathematical modelling provided further evidence supporting the role of crosstalk between $InsP_3R$ and RyRs and the potential for Ca^{2+} release via $InsP_3Rs$ to sensitize RyRs to Ca^{2+}. The increased spontaneous Ca^{2+} spark events contributed to the development of Ca^{2+} waves, which through engaging the sodium Ca^{2+} exchanger, led to cell depolarization and action potential generation. This arrhythmogenic activity was further established in a tissue wedge model where increased arrhythmic activity was detected when perfused with AngII to increase $InsP_3$. The effects of AngII were suppressed by the $InsP_3R$ inhibitor 2-APB. Together, provide a new mechanistic basis for the action of $InsP_3$ mediated Ca^{2+} release in cardiomyocytes, whereby $InsP_3Rs$ in the neighbourhood of RyRs act to tune their sensitivity to Ca^{2+} release. We further identify $InsP_3Rs$ as important players in the pathology of human heart where they promote arrhythmogenic activity and diminished Ca^{2+} transients.

SA10

Epicardial Adipose Tissue as a Modulator of Cardiac Arrhythmogenesis

Ruben Coronel[1]

[1]*Amsterdam University Medical Centres, Amsterdam, Netherlands*

Background: Obesity is a significant risk factor for arrhythmic cardiovascular death. Interactions between Epicardial Adipose Tissue (EAT) and myocytes are thought to play a key role in the development of arrhythmias. Cross talk between EAT and the heart has various component. First, adipose tissue infiltration within the myocardium constitutes an anatomical obstacle to cardiac excitation. It causes activation delay and increases the risk of arrhythmias. Intercellular electrical coupling between cardiomyocytes and adipocytes can further slow conduction and increase the risk of block, favouring reentry and arrhythmias. Finally, EAT secretes multiple substances that influence cardiomyocyte electrophysiology either by modulating ion currents and electrical coupling, or by stimulating fibrosis. However, the effect of EAT secretome (EATs) on cardiac electrophysiology is largely unknown. We investigated the arrhythmogenicity of EAT secretome and its underlying molecular and electrophysiological mechanisms.

Methods: We collected atrial EAT and subcutaneous adipose tissue (SAT) from 30 patients with atrial fibrillation (AF), and EAT from 3 donors without AF. The secretome was collected after a 24-hour incubation of the adipose tissue explants. We cultured neonatal rat ventricular myocytes (NRVMs) with EATs, SAT secretome (SATs) and cardiomyocytes conditioned medium (CCM) for 72H. We implemented the electrophysiological changes observed after EATs incubation into a model of human left atrium and tested *in silico* arrhythmia inducibility.

Results: Cardiomyocytes incubated with EATs showed reduced conduction velocity and increased conduction heterogeneity compared to SATs and CCM. This was associated with a decreased expression of the potassium channel subunit Kcnj2 by 26% and correspondingly reduced the inward rectifier K+ current (IK1) by 35% in comparison to incubation with CCM, and resulted in a depolarized resting membrane of cardiomyocytes. EATs caused decreased expression of connexin43 (29% mRNA, 46% protein) in comparison to CCM. Cells incubated with SATs showed no significant differences in Kcnj2 nor Gja1 expression in comparison to CCM, and their resting membrane was not depolarized. In silico modeling of human left atrium revealed that the electrophysiological changes induced by EATs promote sustained reentrant arrhythmias if EAT partially covers the myocardium.

Conclusion: EAT slows conduction, depolarizes the resting membrane, alters electrical cell-cell coupling and facilitates reentrant arrhythmias.

C01

Intramyocardially implanted engineered heart tissues show intermittent entrainment during the acute post-implantation phase

Eline Huethorst[1], Francis Burton[1], Godfrey Smith[1]

[1]University of Glasgow, Glasgow, United Kingdom

The therapeutic effect of engineered heart tissues (EHTs) is only at its full potential once the EHTs integrate into the native myocardium, and thus electrically and/or mechanically couple. However, the electromechanical coupling of EHTs with the host remains a challenge. The electromechanical cues of the heart might be crucial for EHTs to mechano-electrically couple and this might be especially true for the first couple of hours post-implantation (acute phase), which, to our knowledge, has not been studied.

The aim is to investigate whether small EHTs show signs of mechanical and/or electrical coupling during the acute implantation phase.

Small EHTs consisted of a recombinant collagen hydrogel disc (6 mm x 300 µm thick) with commercial human induced pluripotent stem cell derived cardiomyocytes (hiPSC-CMs) (ICell^2 CDI) seeded on top (<50.000 cells). Hearts of healthy male NZW rabbits were excised under anaesthesia (0.5 ml/kg euthatal with 500U heparin) and prepared for Langendorff perfusion. Blebbistatin was used to block contraction before implanting Cal520-AM loaded EHTs underneath the epicardium. To measure the effect of ventricular contraction, a balloon was inserted into the left ventricle (LV) and hearts were divided into two groups: 1) constant contraction block (CB) using blebbistatin (N=9 hearts) and 2) graded levels of contraction (GC) achieved by washing off the blebbistatin (N=6). Calcium traces (CaT) were recorded alongside the ECG for approximately 30 seconds every 25 mins using a lightguide and traces were categorized into three timepoints post-implantation: Start (T=0), Early (T=20-50mins) and Late (T=70-100mins). The Rayleigh test (1,2) was used to detect potential entrainment based on the distribution of the phase differences between ECG R-wave and CaT. In recordings with significant tendency towards a single phase, runs of 5 or more CaT with delay from the previous R-wave within a 18ms window were considered entrained. Then, entrained parts of the trace were analysed on RR interval, CaT interval, time from the QRS to the CaT upstroke and the ECG:CaT ratio.

CaT could be recorded for multiple hours post-implantation. Contraction was 1.0±0.3% (mean±SD) in the presence of blebbistatin and increased after wash-out to 34.3±20.3% and 85.2±13.3% in the Early and Late groups, respectively (GC group only). The Rayleigh test showed significant result for some traces (12/65 [18.5%] for CB and 11/35 [31.4%] for GC) and this was equally divided between Early and Late timepoints. Furthermore, it appeared that entrainment occurred intermittently (**Figure 1**). Further analysis of entrained trace selections did not show a 1:1 coupling with the heart but often 1:3 or 1:4 and occasionally 1:2, indicating that the human EHTs could not follow the fast intrinsic rate of the rabbit heart.

These data indicate that EHTs show periodic entrainment when engrafted into myocardium in the first hours post-implantation. Entrainment was seen in absence of contraction and therefore contraction seemed not essential. One potential underlying mechanism could be ephaptic

coupling and this hypothesis is currently being tested using a mathematical model. The early phase coupling indicated here may be important for the long-term survival and therapeutic potential of EHTs.

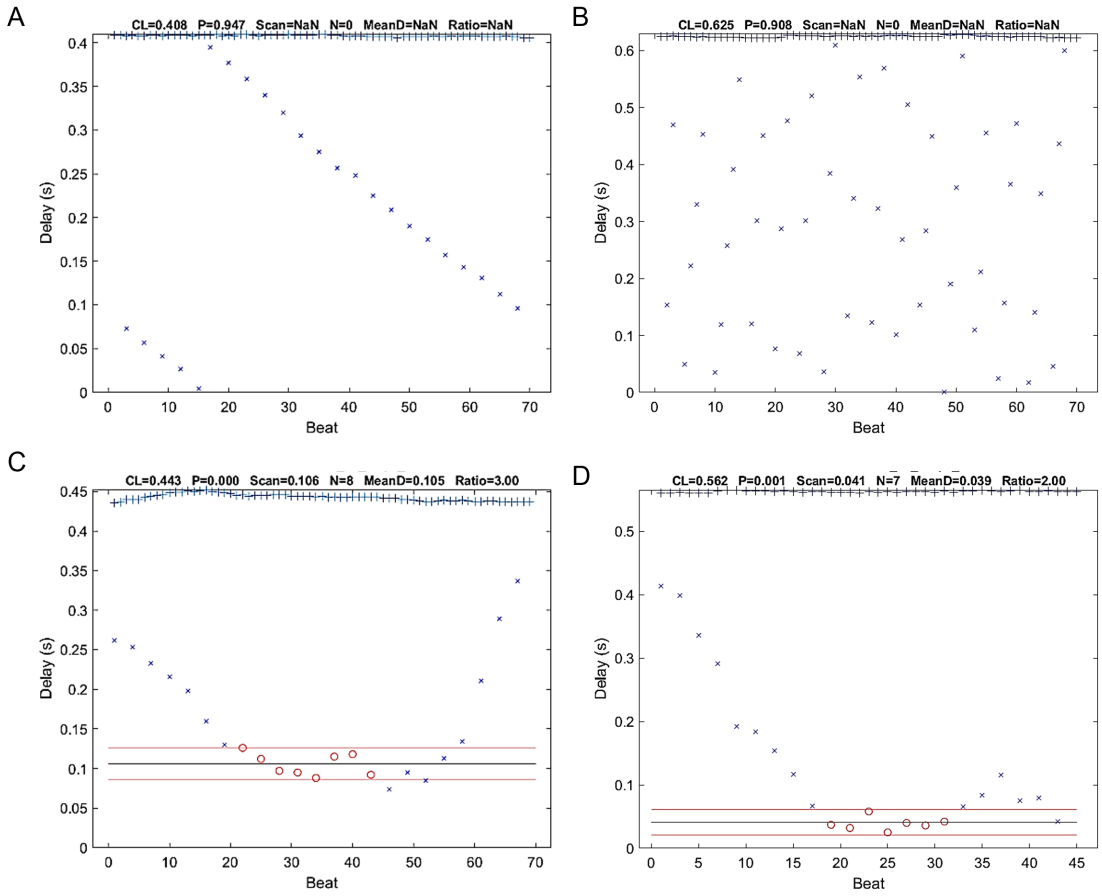

Figure 1 Example graphs of not-entrained (A and B) and entrained (C and D) traces derived from the contraction block group (A and C) and the gradual contraction group (B and D). Graphs show the time points of the QRS complex against the RR interval (+) and the time points of the CaT against the delay (x). Red circles indicate entrained parts of the trace, where the red lines indicate a delay value with a range of ±9ms. CL = cycle length; P = p-value derived from the Rayleigh test where $p<0.05$ means entrained; Scan = the mean delay value of the range; N = number of entrained CaT; MeanD = the mean delay value of the entrained part of the trace; Ratio = ECG:CaT ratio.

1. Fisher, N. (1993). Statistical Analysis of Circular Data. Cambridge: Cambridge University Press. doi:10.1017/CBO9780511564345 2. Berens, P. (2009). CircStat: A MATLAB Toolbox for Circular Statistics. Journal of Statistical Software, 31(10), 1–21. https://doi.org/10.18637/jss.v031.i10

C02

Cardiac ion channel expression profiles in the pulmonary vein of the racing equine athlete with atrial fibrillation

Magdalena Arevalo Turrubiarte[1], Charlotte Edling[1], Bronte Forbes[2], Joe Weir[2], Victoria Kemp[2], Rebecca Lewis[1], Celia Marr[3], Kamalan Jeevaratnam[1]

[1]School of Veterinary Medicine, University of Surrey, Guildford, United Kingdom, [2]The Hong Kong Jockey Club, Sha Tin Racecourse, New territories, Hong Kong, [3]Rossdales Equine Hospital and Diagnostic Centre, Exning, Suffolk, United Kingdom

Background: Atrial fibrillation (AF) is one of the most common causes of cardiac arrhytmia in the heart (1). A relationship between AF and exercise is controversial as exercise seems to protect the heart, in contrast, extremely vigorous long-term exercise could increase cardiac problems (2). AF causes poor performance in horses, and knowledge about the molecular initiation of AF of the pulmonary vein (PV) (3) in the athletic horse is still (4) unknown. Ion channels, responsible for cardiac action potential generation and electrical propagation are target-study of AF causes, in addition to this, the interest in investigating them is because they seem to interact with AF treatments (3). Therefore, this study aims to investigate the molecular ion channel expression pattern in the PV of the athletic horse to get a global gene map expression of this condition.

Methods: Heart samples were obtained from ten horses. Five horses were healthy, and the other five clinically reported suffering AF condition. All ten horses were humanly euthanized due to cardiac affections, and the healthy horses were selected because of musculoskeletal problem- related. Horses belonged to the Hong Kong Jockey Club and were clinically evaluated by veterinarians. Heart tissue biopsies were taken from the left and right atria and ventricle respective sides. Myocardial sleeves from the PV were dissected from the heart. RNA from heart tissue was analysed by RNA sequencing; protein and immunohistochemistry were performed in the samples of healthy and AF horses.

Differential expression of a selection of ion channels and electrophysiological proteins were evaluated. We analysed results by hierarchical clustering and left atrium and PV sequenced samples. PV gene expressions were compared with paired Mann-Whitney-Wilcoxon test. Bioinformatics data and statistics analysis were performed with R software. Results from PV and left atrium samples were clustered separately based on their gene expression. Seven ion channels were significantly ($p<0.05$) increased while six ion channels were significantly under-expressed ($p<0.05$) in the PV sleeves of horses. Gene expression of potassium ion channels such as KCNA4, KCNQ1, KCNH2, KCND3, KCNJ2, KCNN1, KCNN2, and KCNN3 were positively expressed. In addition, calcium-handling proteins (NCX1 and PLN), connexins (CX40), and HCN4 channel ion genes were expressed. Genes in the PV sleeves and left atrium coincide with the differences in the electrophysiological characteristics and conduction velocities. Variations in KCNQ1 and NCX1 genes showed the repolarization patterns of the potassium and calcium homeostasis in the PV sleeves and left atrium. The left atrium and the PV sleeves gene expression showed a specific ion channel pattern of the pulmonary sleeves in the horse.

Conclusion: Our findings show that PV sleeves in athletic horses could initiate AF, this was observed by gene and molecular expression patterns. Therefore, the study of the PV in racing horses using bioinformatics tools analyses could help us clarify relevant biological data and provide us with an understanding location gene map. This study focuses on cardiac dysrhythmias as AF in athlete horses will provide knowledge in human athlete's studies due to similarities in ion channel expression patterns.

C03

Small extracellular vesicles released by cardiac fibroblasts from hypertrophic cardiomyopathy patients alter action potential of human cardiomyocytes

Georgina Thompson[2], Elias Suliman[1], Konstantinos Savvatis[3], Sean Davidson[1], Aled Clayton[4], John McVey[2], Patrizia Camelliti[2]

[1]The Hatter Cardiovascular Institute, University College, London, United Kingdom, [2]School of Biosciences and Medicine, University of Surrey, Guildford, United Kingdom, [3]Inherited Cardiovascular Diseases Unit, Barts Heart Centre, London, United Kingdom, [4]Division of Cancer & Genetics, Cardiff University, Cardiff, United Kingdom

Cardiac fibroblasts (CFs) are abundant in the heart, where they play a major role in cardiac homeostasis and disease development (1). Recently, small extracellular vesicles (sEV) released by mouse CFs have been implicated in cardiac hypertrophy (2). However, if human CF sEV have a role in cardiac disease remains unclear. Here we isolate CFs from hypertrophic cardiomyopathy (HCM) patients, purify and characterise their sEV and study the effect of these sEV on Ca^{2+} cycling and action potentials of human cardiomyocytes (CMs).

CFs isolated from HCM patients' biopsies were characterised by RT-qPCR, flow cytometry and immunohistochemistry. Media conditioned by CFs over 72 hours was concentrated by ultrafiltration. sEV were purified by size exclusion chromatography and characterised by nanoparticle tracking analysis and tetraspanin staining, purity was determined using microBCA. CMs were differentiated from human induced pluripotent stem cells and cultured for 28 days before purification using MACS bead separation. Purified CMs were cultured with sEV from HCM CFs for 48 hours. Action potentials and calcium (Ca^{2+}) transients were studied using optical mapping, with calcium dye (Fluo-4) or voltage dye (FluoVolt), during field stimulation at 0.7Hz, 1Hz and 1.5Hz. Signals were analysed using OPTIQ software. Unpaired T-tests were used for statistical analysis of 2 groups.

CFs from HCM patient biopsies had a myofibroblast pheno/genotype determined by the presence of myofibroblast markers: α-SMA, COL1A1, FAP. Pure sEV were found in fractions 7-9 (>$2x10^{10}$ particles/μg), had a modal size of 109±3.5nm and were positive for the tetraspanins CD63, CD81 and CD9. On average HCM CFs secreted 104,676 sEV per cell (n=3). CM Ca^{2+} transient parameters, time to peak and time to 50/80% Ca^{2+} decay, were unaffected by HCM CF sEV at a concentration of $5x10^{10}$ particles/ml ($p>0.05$ vs untreated CM, n=4). However, CM action potentials were prolonged after culture with HCM CF sEV at a concentration of $5x10^{10}$ particles/ml with a significant increase in action potential duration (APD)50 at 1Hz ($p<0.01$ vs untreated CM), 0.7Hz and 1.5Hz ($p<0.05$); and significant increase in APD80 at 1Hz and 0.7Hz ($p<0.01$) and 1.5Hz ($p<0.05$, n=4).

Our results indicate that CFs isolated from HCM patients have a myofibroblast phenotype and secrete a large number sEV. Treating human CMs with highly pure sEV secreted by HCM CFs prolongs CM action potential duration, highlighting a potential role of CF sEV in heart disease.

1. Souders CA, Bowers SLK, Baudino TA. Cardiac fibroblast: The renaissance cell. Circ Res. 2009;105(12):1164–76. 2. Bang C, Batkai S, Dangwal S, Gupta SK, Foinquinos A, Holzmann A,

et al. Cardiac fibroblast-derived microRNA passenger strand-enriched exosomes mediate cardiomyocyte hypertrophy. J Clin Invest. 2014;124(5):2136–46.

C04

Calcium signalling in cardiac fibroblast and myocytes in an in vitro model of heart failure with preserved ejection fraction.

Zainab Olatunji[1], Susan Currie[2], Niall MacQuaide[1]

[1]Department of Biological and Biomedical Sciences, Glasgow Caledonian University, Glasgow, United Kingdom, [2]Strathclyde Institute of Pharmacy & Biomedical Sciences, University of Strathclyde, Glasgow, United Kingdom

Introduction:

Heart Failure with preserved Ejection Fraction [HFpEF] is a pandemic associated with hypertension and diabetes amongst other co-morbidities. It has been established that fibrosis plays a major role in this form of heart failure. However, the functional mechanisms of cardiac fibroblasts (CFs) in HFpEF and more importantly, how these cells interact with cardiomyocytes (CMs) and impact calcium (Ca^{2+}) signalling is limited. This limitation is majorly due to a lack of physiologically relevant cellular models.

Aims/Objectives:

To study the CF-CM interaction in an *in vitro* model of HFpEF, this study aimed to evaluate the Ca^{2+} response of CFs in diabetic, hypertensive, and HFpEF conditions. Furthermore, the electrophysiology of CMs co-cultured with CFs, under these pathological conditions was assessed.

Methods:

Adult human male CFs (HcFb) (Promocell) at Passage 3 were seeded at a density of $1x10^4$ cells per well in a 96-well plate and grown for 24 hours in fibroblast growth medium 3 (FGM3) supplemented with 10% Foetal Calf Serum (FCS) and 1% Penicillin/Streptomycin (P/S). Cells were serum starved for 24 hours prior to treatment. For CFs Ca^{2+} signalling, fibroblasts were treated for 72 hours with high glucose (22mM) to simulate diabetes, high Angiotensin-II (Ang-II) (200nM) to simulate hypertension, or both conditions to simulate HFpEF. Cells were stained with 2μM Cal520 AM calcium indicator and the Ca^{2+} response induced by the addition of 20nM Endothelin-1 was measured by confocal microscopy. For co-culture, adult male rabbit CMs were freshly isolated following all ethical requirements by the UK Home Office Licence. CMs were cultured with(out) CFs in either Medium 199 (M199) or FGM3, using treatment conditions similar to the above. Following treatment, CMs were harvested, stained, and electrically stimulated at 1Hz to measure single cell Ca^{2+} transients.

Results:

The Ca^{2+} transient amplitude of CMs was significantly reduced when cultured in FGM3 or co-cultured with HcFb in M199, compared to M199 (M199: 0.766±0.112 versus FGM3: 0.145±0.0266; co-cultured myocytes in M199: 0.347±0.0385, N=1 rabbit and n≥5 cells per group; $p< 0.001$, one-way ANOVA). Endothelin-1-induced Ca^{2+} response in CFs was significantly enhanced with high glucose when compared to control, hypertensive and HFpEF

conditions (Control: 3.67±1.32 versus Diabetic: 13.7±1.34; Hypertensive: 6.29±1.04; HFpEF: 7.14±1.27, N=2 biological replicates with n=3 technical replicates each; $p< 0.05$, one-way ANOVA). Using the same treatment conditions, similar effects on Ca^{2+} transient amplitude were observed in electrically stimulated co-cultured CMs. (Control: 0.294±0.0164 versus Diabetic: 0.716±0.108; Hypertensive: 0.611±0.0935; HFpEF: 0.546±0.0460, N=1 rabbit and n≥5 cells per group; $p< 0.05$, one-way ANOVA). These results are contrary to existing data that show no significant change in Ca^{2+} transient amplitude of CMs treated with high glucose and increased amplitude with high Ang-II treatment.

Conclusions:

Ultimately, these findings suggest different regulation of Ca^{2+} by CFs during hypertension and HFpEF when compared with that seen during diabetes. Furthermore, data indicate a notable influence of CFs on CM Ca^{2+} transient amplitude. Ongoing work is exploring the role and mode of intercellular communication by both cell types in cardiomyopathy.

C05

Chronic myocardial infarction attenuates transmural heterogeneities but alters the response to endothelin and β-adrenergic stimulation in porcine ventricles

Alba Pérez Martínez[1], Cristina López-Andres[1], Cristina Pastor[3], Esther Pueyo[1,2], Aida Oliván-Viguera[1,2]

[1]Universidad de Zaragoza, Zaragoza, Spain, [2]CIBERBBN, Zaragoza, Spain, [3]Instituto Aragonés de Ciencias de la Salud (IACS), Zaragoza, Spain

Increased susceptibility to ventricular arrhythmias is well documented after myocardial infarction (MI). There is consistent evidence supporting differences in transmural and apicobasal repolarization gradients as substrates for ventricular tachycardia and arrhythmogenesis. Nonetheless, there is limited direct evidence on how post infarct dynamics may differentially affect transmural regions in the heterogeneous peri-infarct zone. Information on how different cell types contribute to an arrhythmogenic electrophysiological profile is also scarce.

Aim: To assess the effects of chronic MI on centre-to-base and transmural repolarization gradients at baseline and in response to adrenergic stimulation (isoproterenol) and endothelial factors (endothelin-1, ET-1).

Methods: Domestic pigs (n=5) were infarcted by temporal occlusion of the left circumflex (LCx) coronary artery. 7-12 weeks after infarct induction, animals were cardioplegically arrested under deep anaesthesia and sacrificed. Healthy pigs (n=11) were used as controls. All animal procedures conformed to the guidelines from Directive 2010/63/EU and were approved by local authorities. Ventricular slices were produced form transmural tissue blocks obtained from remote and adjacent zones of the infarct area at the base and in the centre of the ventricular wall. Same areas of the ventricle from healthy pigs were taken as controls. Slices from the endocardium, midmyocardium and epicardium were optically mapped to record transmembrane potential. Action Potential Duration (APD) was measured at 80% repolarization at 1Hz pacing frequency at baseline conditions and after the addition of 100 nM isoproterenol or 100 nM ET-1 .

Results: Transmural heterogeneities in APD80 at basal conditions were attenuated in the infarcted tissue. Endocardial and epicardial tissue presented APD80 prolongation at the base of the infarcted hearts, especially in the areas adjacent to the infarct, while the midmyocardial tissue presented a slightly decreased APD80. At the centre, APD80 was decreased in all layers of the transmural wall, but this effect was more pronounced in the midmyocardial areas adjacent to the infarct. ET-1 prolonged APD80 by 38% (endo), 13% (mid) and 20% (endo) at the base and by 28%, 17% and 5% at the centre. Such a response was enhanced at the base in the areas adjacent to the infarct (63%, 40% and 15%) and maintained in the remote areas (14%, 18% and -3%). At the centre, the response to ET-1 was slightly diminished in the adjacent areas (3%, 25% and 5%). Isoproterenol shortened APD80 by 8% (mid) and 5% (epi) at the base and by 14% and 17% at the centre of healthy ventricles. There was a very mild response, however, at the base of the infarcted hearts (remote +1% and -3% and adjacent +5% and +11%), and the response in the centre was inverted (remote +19% and +18% and adjacent +8 and +0%).

Conclusions: Chronic MI by occlusion of LCx in pigs leads to attenuation of transmural heterogeneities, spatially heterogeneous response to adrenergic stimulation and increased

sensibility to ET-1. All these factors may indicate increased susceptibility to ventricular arrhythmias. Future studies of the mechanisms underlying the here described transmural heterogeneous remodelling in MI would lead to improved antiarrhythmic therapies.

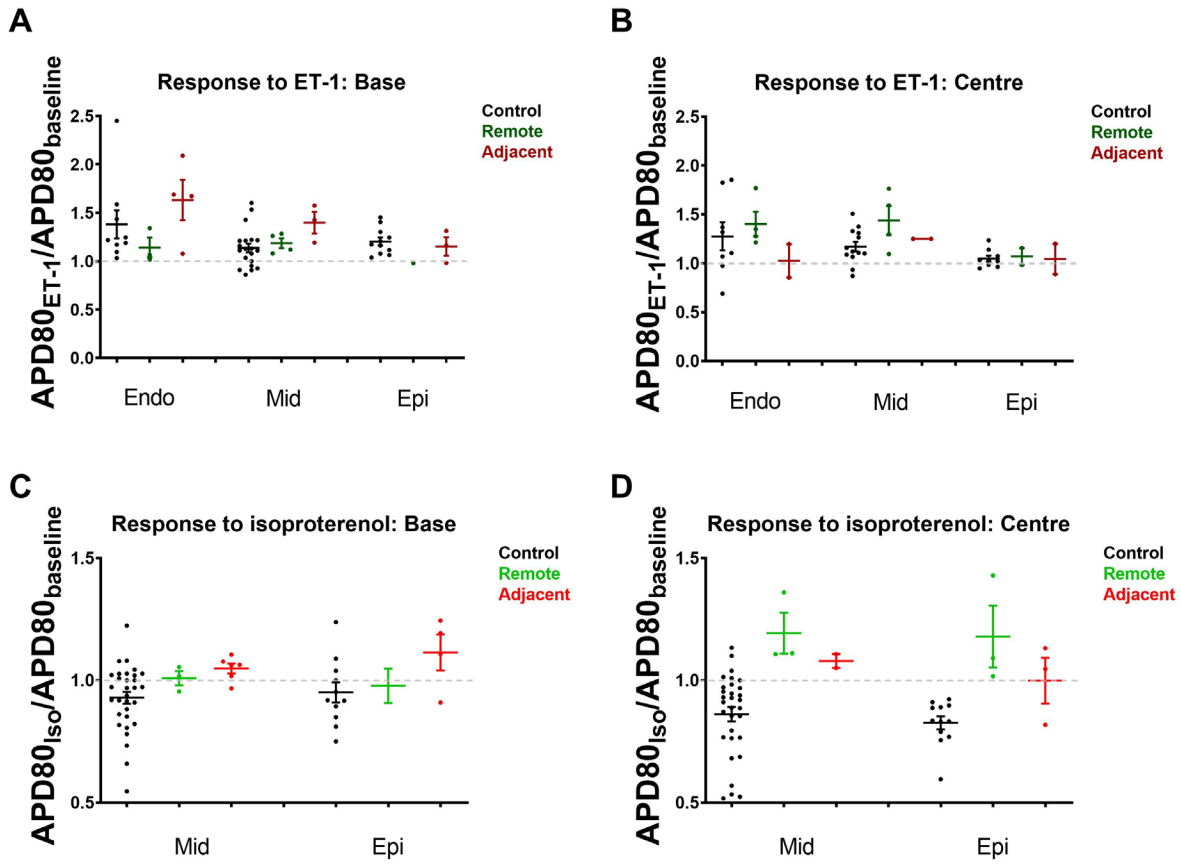

- Dries E, Amoni M, Vandenberk B, Johnson DM, Gilbert G, Nagaraju CK, et al. Altered adrenergic response in myocytes bordering a chronic myocardial infarction underlies in vivo triggered activity and repolarization instability. J Physiol. 2020;598(14):2875–95. Sung E, Prakosa A, Trayanova NA. Analyzing the Role of Repolarization Gradients in Post-infarct Ventricular Tachycardia Dynamics Using Patient-Specific Computational Heart Models. Front Physiol. 2021;12(September).

C06

Investigating the effect of substrate stiffness on iPSC-CM structure and function

Leena Patel[1], Daniel Tennant[1], Katja Gehmlich[1]

[1]University of Birmingham, Birmingham, United Kingdom

Introduction:

Cardiac ageing is characterised by increased stiffness of the myocardium, due to excess deposition of extracellular matrix (ECM) proteins such as collagen. The structural remodelling of the myocardium can consequently impact the behaviour of surrounding cells, such as cardiomyocytes (CMs). Current research using induced pluripotent stem-cell derived cardiomyocytes (iPSC-CMs) may not truly reflect the physiological stiffness of the ECM in healthy or diseased conditions. In order to assess the effect of ECM stiffness on iPSC-CMs structure and metabolic function, polydimethylsiloxane (PDMS) substrates can be used to recapitulate healthy (20kPa) and fibrotic (130kPa) stiffnesses.

Aims:

To investigate differences in structure and function of iPSC-CMs on soft and stiff PDMS substrates.

To explore changes in iPSC-CM metabolism on substrate stiffnesses.

Materials and Methods:

iPSC-CMs were plated onto PDMS gels of 20kPa and 130kPa and harvested between days 20-30 of differentiation. Molecular analyses of iPSC-CMs were investigated using qPCR, western blotting and immunofluorescence to explore cardiac gene expression profiles and structural parameters such as sarcomere length and actin organisation. Contractility of iPSC-CMs on stiffnesses were assessed using MuscleMotion software, which utilised video recordings of cells from a GoPro. Isotope labelled mass spectrometry was conducted on iPSC-CMs on varying stiffnesses to explore changes in metabolic pathways, as well as metabolic gene expression changes.

Results: Softer substrates induce maturation of iPSC-CMs, with significantly higher expression of cardiac maturity markers such as MYH7:MYH6 ratios and MYL2:MYL7 ratio compared to stiffer plastic conditions. Maturation is further displayed on 20kPa PDMS, with iPSC-CMs portraying a higher level of sarcomere alignment compared to plastic and 130kPa. Contractility of iPSC-CMs is altered on softer substrates. Metabolic profiles of iPSC-CM on stiffer gels display higher glycolytic metabolites such as glucose, whereas cells on softer substrates portray TCA cycle metabolites.

Conclusions: Substrate stiffnesses can act as physiological models of healthy and diseased ECM by portraying molecular changes in iPSC-CM structure and maturity, as well as recapitulating switches in iPSC-CM metabolism.

C07

Adrenergic modulation of ventricular transmural conduction velocity is a novel factor governing electrical excitability in health and disease.

Erin Boland[1], Francis Burton[1], Sasha Forbes[1], Godfrey Smith[1]

[1]School of Cardiovascular and Metabolic Health, University of Glasgow, Glasgow, United Kingdom

Introduction - Conduction velocity (CV) is an important determinant of the arrhythmic status of the ventricle. SNS-mediated changes in CV may contribute to the normal ventricular activation sequence. We utilised a custom-made electrode array to record epicardial electrograms at sites in longitudinal, transverse, and transmural directions that incorporates a light guide to allow optical AP measurements from the electrogram recording area (**Fig. 1**). This set-up allows beat-to-beat assessment of myocyte to myocyte conduction and electrophysiological parameters to examine the magnitude and time course of pharmacologically mediated changes targeting the adrenergic signalling pathway. It has been well established that β-adrenoceptor expression and sympathetic nerve remodelling are pathological features of heart failure. Our approach will resolve CV changes in response to adrenergic modulation initially in the healthy heart which will then form the basis of our comparison to adrenergic signalling post-MI.

Methods - The hearts of adult, male New Zealand White rabbits were rapidly excised following terminal Euthatal administration via marginal ear vein according to UK Home Office approval and legislation. Hearts were Langendorff-perfused at 37°C and perfused with the voltage sensitive dye FluoVolt™ to record APs. For transmural recordings, an electrode was then inserted via the left atria into the LV and placed against the endocardial surface of the mid LV free wall at a corresponding point to the endocardial electrode to measure transmural conduction velocity (CVtm). The custom endocardial electrode comprised of a pair of stimulating electrodes and two pairs of recording electrodes at a 90° angle from each other corresponding to the longitudinal (CVl) and transverse (CVt) epicardial fibre orientation. Each CVl and CVt recording electrodes were spaced at a 2mm distance and used to calculate epicardial conduction velocity. To calculate CVtm, the thickness of the LV mid-wall was determined post-experiment.

Results - The high sampling rates (20kHz) enabled us to document small electrophysiological changes including alternans in both AP and CV measurements. Thus far, we have resolved CV and APD changes as small as 1%. 100nM Isoprenaline elicits an increase in CVl (13.2%), CVt (14.4%), and CVtm (12.8%) with a corresponding decrease in APD90 of -16.5% (n=8). Interestingly, increasing intracellular Ca^{2+}, a known effect of SNS activation, via infusion of 5mM Ca^{2+} resulted in a reduction in CVl (-13.0%), CVt (-11.0%), and CVtm (-9.0%) with a corresponding decrease in APD90 of -9.1% (n=5). Mimicking SNS activation by raising increasing intracellular cAMP via 15μM Forskolin and 50μM IBMX, a similar pattern emerged of CV and APD changes as Isoprenaline in CVl (11.1%), CVt (12.1%), CVtm (10.66%), and APD90 (-13.20%) (n=8). These findings also suggest that the increase in CV brought about by

adrenergic stimulation must also overcome the reduction in CV which is a result of increased intracellular Ca^{2+}.

Conclusions - By utilising this novel electrode and light guide system, we have begun to establish the effect of adrenergic signaling on the interplay between increased myocyte to myocyte conduction velocity and action potential characteristics at a resolution not previously achieved.

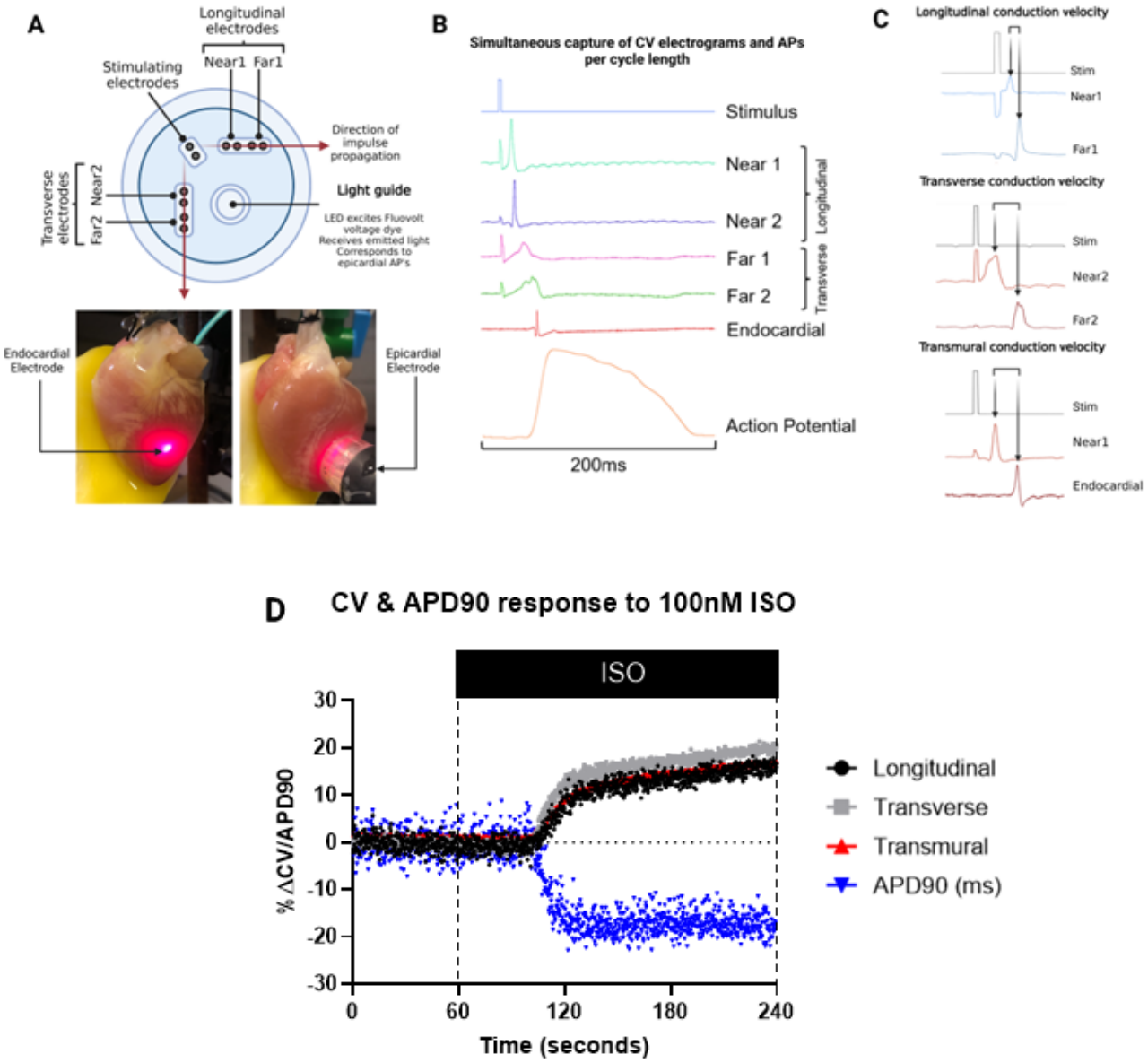

Figure 1. Custom epicardial and endocardial electrode design and recordings. (**A**) Orientation of bipolar stimulating electrode, two pairs of longitudinal and transverse recording electrodes, and light guide within the epicardial surface electrode. Also shown is the endocardial electrode consisting of a light guide for position visualisation (not used during data acquisition) and a pair of recording electrodes passed into the LV via the mitral valve and contacting the endocardial surface perpendicular to the epicardial electrodes. (**B**) Example recording from one cycle length duration (endocardial pacing via surface bipolar electrode at 190ms) demonstrating simultaneous capture of longitudinal, transverse, transmural and APs aligned to 2ms stimulus pulse. (**C**) Calculation of longitudinal (**CVl**), transverse (**CVt**), and transmural (**CVtm**) conduction velocity from epicardial and endocardial electrograms using the AnalyseCVElectrograms software developed by Francis Burton. (**D**) Example beat-to-beat recording of CVl, CVt, CVtm, and APD90 following 3-minute infusion of 100nM Isoprenaline.

C08

Development of a human model of parasympathetic neurons and atrial cardiomyocytes

Laura Fedele[1], Alison Thomas[2], Franziska Denk*[3], Andrew Tinker*[2]

[1]Wolfson Centre for Age-related Diseases, King's College London, Guy's Campus, London, SE1 1UL, UK, London, United Kingdom, [2]Clinical Pharmacology & Precision Medicine, William Harvey Research Institute, Barts and the London School of Medicine and Dentistry, Queen Mary University of London, London, UK, London, United Kingdom, [3]Wolfson Centre for Age-related Diseases, King's College London, Guy's Campus, London, SE1 1UL, UK, London, United Kingdom

INTRODUCTION: The cardiac autonomic nervous system regulates the heart intrinsic activity (e.g., heart rate), and its dysregulation is involved in a number of cardiac arrhythmias. Dysfunction of parasympathetic neurons has been associated with atrial fibrillation, the most common form of cardiac arrhythmias (2.5% of English population [1]). Unfortunately, the interaction between parasympathetic neurons and atrial cardiomyocytes is particularly difficult to study and, to our knowledge, there are currently no human *in vitro* models.

AIMS: Our project aims to develop a human *in vitro* model of the interaction between parasympathetic neurons and atrial cardiomyocytes. It will allow us to investigate the cross-talk between these cells, to manipulate them to study atrial fibrillation (e.g. through genetic manipulation) or to carry out drug screening work.

METHODS: We have generated atrial cardiomyocytes and parasympathetic neurons from induced pluripotent stem cells. We followed published protocols for atrial cardiomyocytes [2] and parasympathetic (vagal) neurons [3]. With a combination of immunostaining and functional recordings (e.g. Ca^{2+} imaging and patch clamp recordings) we characterised the neurons confirming their function and lineage. Using qPCR and immunostaining we compared the expression of atrial and ventricular specific markers between atrial iPSC-derived cardiomyocytes and standard iPSC-derived cardiomyocytes (Burridge protocol [4]). We co-cultured atrial cardiomyocytes and parasympathetic neurons for 5-7 days and assessed the modulation of cardiomyocyte beating rates by the activation of the neurons with nicotine. We also tested whether the effect could be reversed by a neuronal blocker (a selective Nav1.8 antagonist).

RESULTS: Our data confirm the parasympathetic nature of the iPSC-derived neurons, as they express the autonomic lineage marker Phox2b and the cholinergic marker ChAT. They are also responsive to nicotine, as expected. Atrial iPSC-derived cardiomyocytes present a reduction in ventricular specific markers (e.g. MYL2, IRX4 assessed with qPCR) and increased expression of atrial markers with immunostaining (e.g. MYL7).

When we cocultured the two cell types for 7 days, nicotine (20μM) resulted in a significant reduction of cardiomyocyte beating rate in co-cultures compared to mono-cultures (mono-culture: 111.2±2.729; co-culture: 65.42±6.931; p=0.002; Mann-Whitney test; n= 6 two differentiations of the parasympathetic neurons). Interestingly, the activity-dependent Nav1.8 blocker A803467 (100nM) increased the beating rate in co-culture but not in mono-culture

(mono-culture=96.28±0.7658; co-culture=130.8±11.09; *p*=0.0043; Mann-Whitney test; n=6; two differentiations of the parasympathetic neurons) reversing, to some extent, the effect of nicotine.

CONCLUSIONS: Our preliminary data show a potential to reproduce *in vitro* some key physiological features of parasympathetic neurons-cardiomyocyte interactions. In future studies, we aim to extend our characterisation and employ our system for disease modelling.

1.https://cks.nice.org.uk/topics/atrial-fibrillation/background-information/prevalence/ 2.Cyganek et al (2018) JCI Insight 21;3(12):e99941 3.Maury et al (2015) Nat Biotechnol 33(1):89-96 4.Burridge et al (2014) Nat Methods. 2014;11(8):855–860

C09

A novel electrophysiological approach to investigate sympathetic autonomic ganglia in Parkinson's Disease Animal Model: a loose-patch clamp.

Bonn Lee[1], Shiraz Ahmad[1], Charlotte Edling[1], Fiona LeBeau[2], Kamalan Jeevaratnam[1]

[1]School of Veterinary Medicine, Faculty of Health and Medical Sciences, University of Surrey, Guildford, United Kingdom, [2]Biosciences Institute, Faculty of Medical Sciences, Newcastle University, Newcastle, United Kingdom

Stellate ganglia (SG) are sympathetic autonomic ganglia that provide sympathetic nerve inputs into the heart and may predispose the myocardial conducting system to atrial and ventricular arrhythmias. In recent years studies have shown a correlation between Parkinson's disease (PD) and cardiac disease which imply autonomic dysregulation in PD. A30P point mutation of alpha-synuclein is a well-established risk factor in PD; A30P mutant alpha-synuclein mouse recapitulates systemically presenting alpha-synucleinopathy. We aim to investigate histological and electrophysiological properties of the stellate ganglia in light of alpha-synucleinopathy in PD.

Firstly, we here demonstrate that A30P mutant alpha-synuclein is expressed in the sympathetic adrenergic cells in stellate ganglia in the PD animal model. This finding contradicts Braak's hypothesis that canonically regards the vagal nerve as the primary gateway of alpha-synuclein propagation. Secondly, we have developed a technique to patch stellate ganglionic tissue for electrophysiological examination and we here present sodium and potassium channel properties of murine stellate ganglia.

To investigate further, we aim to study the electrophysiology of stellate ganglia in A30P mutant mice, which will help explain the increased risk of cardiac dysautonomia in PD.

Kahle, P. J. et al. (2000), J. Neurosci, 20(17), 6365-6373. Rajendran, P. S.et al. (2019), Nat Commun, 10(1), 1944.

C10

SYMPATHETIC NERVOUS REGULATION OF VENTRICULAR FIBRILLATION IN GUINEA PIG HEARTS

Christopher O'Shea[1], James Winter[1], Davor Pavlovic[1]

[1]University of Birmingham, Birmingham, United Kingdom

Background: Sympathetic nervous stimulation (SNS) exerts critical effects on cardiac electrophysiology. Several reports have investigated whether SNS suppresses or promotes the onset of ventricular fibrillation (VF). However, is not known whether SNS alters the dynamics of VF once it is initiated. Recent optical mapping studies have revealed a wide spectrum of mechanisms that drive and sustain VF. Fibrillation mechanisms have important consequences for treatment options, for example whether targeted ablation or pharmacological treatment is optimal for preventing recurrence in VF survivors.

Methods and Results: The epicardial ventricular surface of innervated guinea pig hearts (n=8) were optically mapped at high resolution using voltage dye Rh-237. VF was induced by a dynamic S1 pacing protocol with incrementally shortening cycle length, starting at 170ms. VF was induced with and without bilateral SNS by direct stimulation of efferent sympathetic nerves in the spinal cord.

SNS shortened action potential duration, increased dispersion of repolarisation, and increased conduction velocity. Rotational activity during VF was quantified by the detection and tracking of phase singularities (PS). During SNS, the incidence of stable PSs (>2 rotations) increased by 51±13% ($P<0.01$). SNS also increased the time a stable PS was present during VF from 32±3% to 41±2% ($P<0.01$). Although SNS increased the number of PSs, it did not alter the dynamics of specific PSs such as the number of rotations, lifetime, or spatial spread. In control and SNS conditions, PSs survived for 275±30ms and 310±44ms respectively.

Conclusion: SNS increases the number of transient rotational drivers during VF. Our findings suggest SNS favours multiple stable wavelets driving fibrillation in cardiac tissue, rather than the presence of one ‘Mother Wave’. With modulation of SNS common in several pathophysiological states and treatment options, these results may hold important consequences for the clinical treatment of VF.

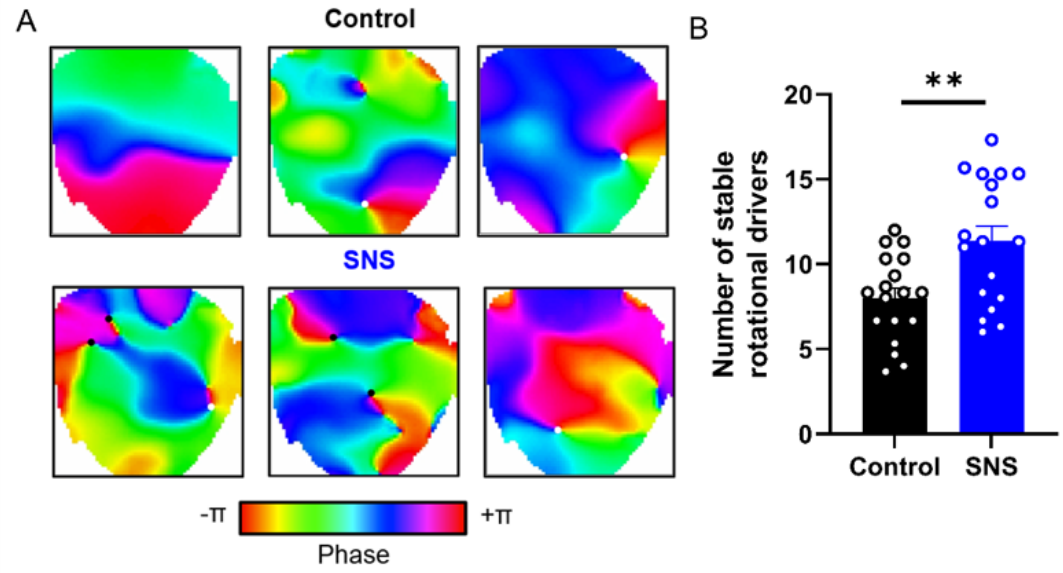

Figure 1: A) Example phase maps during ventricular fibrillation. Black and white dots show identified phase singularities. B) Grouped data showing number of phase singularities in control (black) and SNS conditions (blue) during ventricular fibrillation.

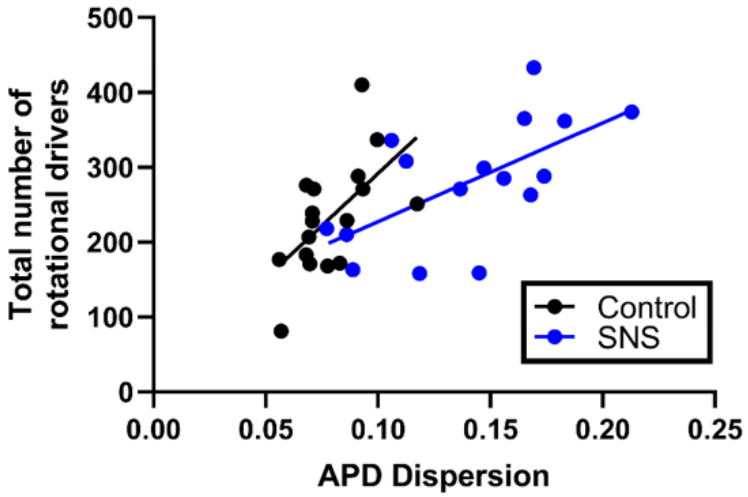

Figure 2: Correlation between APD dispersion during pacing (160ms pacing cycle length) and number of rotational drivers observed during ventricular fibrillation.

C11

Do plasma cytokine levels correlate to cardiac function in coronary artery disease?

Bethan Samphire-Noden[1], Alicia Staley[1], Anna Borun[1], Courtney Riley[1], Sarah Withers[1], Vasanthi Vasudevan[2], Mohamad Nidal Bittar[2], David Greensmith[1]

[1]Biomedical Research Centre, School of Science, Engineering and Environment, The University of Salford, Manchester, M5 4WT, Manchester, United Kingdom, [2]Lancashire Cardiac Centre, Blackpool Victoria Hospital, FY3 8NR, Blackpool, United Kingdom

Coronary artery disease (CAD) affects over 20 million people worldwide and is the leading cause of morbidity and mortality[1]. In CAD, atherosclerosis narrows the coronary arteries leading to myocardial ischemia thence decreased systolic and diastolic cardiac function. Furthermore, previous studies highlight an association between CAD and atrial fibrillation (AF)[2]. The pathogenic mechanisms are complex, though elevations of inflammatory markers such as cytokines play a key role. However, clinical studies examining this are limited[3]. In this preliminary study, we measured plasma levels of cytokines in a CAD patient cohort then correlated those levels to indices of systolic and diastolic cardiac function.

The study was conducted in accordance with local and IRAS ethical approval (IRAS ID: 247341). Preoperative serum samples were collected from patients scheduled for routine coronary revascularisation surgery. Serum interleukin-6 (IL-6), interleukin-10 (IL-10), interleukin-1ß (IL-1ß) and tumour necrosis factor alpha (TNF-a) concentrations were measured using high-sensitivity ELISA kits (Abcam, UK & Invitrogen, USA). Statistical significance was taken when $p < 0.05$ and calculated using Pearson R correlation.

Average IL-6, IL-1ß, IL-10 and TNF-a concentrations were 15.20 ± 1.36, 1.46 ± 0.26, 4.21 ± 0.59 and 2.70 ± 0.61 pg/mL, respectively. We found no significant correlations between the levels of these cytokines and the indices of systolic function measured (EF, LVOT, TASPE, PASP). When cytokine levels were correlated to indices of diastolic function, IL-1ß and IL-10 correlated with peak E-wave velocity (IL-1ß: $p = 0.02$, $r^2 = 0.21$, $n = 27$. IL-10: $p = 0.04$, $r^2 = 0.08$, $n = 53$). No correlations between cytokine levels and end diastolic volume were observed.

These *preliminary* data indicate that levels of IL-1ß and IL-10 correlate to certain indices of cardiac diastolic function so *may* be of use as a prognostic marker in CAD patients. Further experiments will increase study power and seek to identify other key correlates including risk of arrythmia such as AF.

1. Centres for Disease Control and Prevention. (2023). Heart disease statistics and maps. https://www.cdc.gov/heartdisease/statistical_reports.htm 2. Kralev, S., Schneider, K., Lang, S., Süselbeck, T., & Borggrefe, M. (2011). Incidence and severity of coronary artery disease in patients with atrial fibrillation undergoing first-time coronary angiography. PloS one, 6(9), e24964. 3. Kaptoge, S., Seshasai, S. R., Gao, P., Freitag, D. F., Butterworth, A. S., Borglykke, A., Di Angelantonio, E., Gudnason, V., Rumley, A., Lowe, G. D., Jørgensen, T., & Danesh, J. (2014). Inflammatory cytokines and risk of coronary heart disease: new prospective study and updated meta-analysis. European heart journal, 35(9), 578–589.

C12

The effect of MOTS-c on inflammation related cytokines in cardiac and abdominal aortic tissue in abdominal aortic constriction induced cardiac hypertrophy model in rat

Gulsun Memi[1], Ibrahim Turkel[2,3], Ebru Annac[4], Burak Yazgan[5]

[1]Department of Physiology, School of Medicine, Adıyaman University, 02040, Adıyaman, Turkey, [2]Department of Exercise and Sport Sciences, Faculty of Sport Sciences, Hacettepe University, 06800, Ankara, Turkey, [3]3Division of Sport Sciences and Technology, Institute of Health Sciences, Hacettepe University, 06800,, Ankara, Turkey, [4]Department of Histology-Embryology, School of Medicine, Adıyaman University, 02040,, Adiyaman, Turkey, [5]Department of Medical Services and Techniques, Sabuncuoglu Serefeddin Health Services Vocational School, Amasya University, 05100,, Amasya, Turkey

Introduction: Cardiovascular diseases (CVDs) are a set of disorders combined with vascular and cardiac functions such as cerebrovascular disease, angina, atherosclerosis, coronary heart disease, myocardial infarction, and heart failure. CVDs are the most important cause of mortality and morbidity in both developing and developed countries. While acute inflammation is a process that protects tissues, it's becoming chronic and causes various pathologies. CVDs are a chronic inflammatory process. Pro-inflammatory cytokines such as IL-1β, IL-6, IL-17, IL-18, IL-21, IL-33, and TNF-α also trigger pathological disease, however, anti-inflammatory cytokines such as IL-10 and TGF-β reduce inflammation. MOTS-c is a mitochondrial-derived peptide encoded from 12S rRNA in mitochondrial DNA and referred to as the mitochondrial open reading frame of 12S Rna-type c. MOTS-c regulates metabolic pathways such as insulin sensitivity, glucose, and lipid homeostasis. It is stated that MOTS-c has a protective role in the progression of diabetes, cardiovascular disease, inflammation, osteoporosis, aging, and lung injury. However, few studies have investigated the effects of MOTS-c on inflammation.

Objective: We aimed to investigate how MOTS-c affects inflammatory cytokine levels after abdominal aortic constriction (AAC) induced cardiac hypertrophy.

Method: For this purpose, twenty-eight male Wistar albino rats grouped as (aged 2 months) sham+saline (saline;1 ml/kg, n=6), sham+MOTS-c (MOTS-c;5 mg/kg,n=6), AAC+saline(Saline;1 ml/kg,n=8) and AAC+MOTS-c (MOTS-c;5 mg/kg,n=8). Cardiac hypertrophy models were induced by abdominal aortic ligation by using 4.0 silk sutures (Marano G,et al., 2002). Following the formation of the AAC model for 14 days, treatments were administered intraperitoneally for 21 days. Under ketamine+xylazine (100 mg/kg+15 mg/kg; i.p) anesthesia the rats were sacrificed and serum and tissue samples were taken. Histopathological analyses were performed with hematoxylin-eosin, Masson's trichrome, and Toluidine blue in the thoracic and abdominal aorta and heart tissue. The mRNA expressions of IL-1β, IL-18, TGF-β, and TNF-α genes involved in the inflammatory process in both the left ventricle of the heart and abdominal aorta tissues were determined by qPCR. Data were given as mean ± standard error, statistical analysis was compared with t-tests in independent groups. All experiments were performed in accordance with the "Animal Welfare Act and the Guide for the Care and Use of Laboratory Animals prepared by the Adiyaman University, Animal Ethical Committee"(Turkey (Approved date 04.11.2022, no;2021/030).

Result: Histopathological analyses showed that the abdominal aortic tissue deteriorated in the AAC+saline group, while the vessel wall structure of the AAC+ MOTS-c treatment group was preserved.

mRNA expressions of IL-1β, IL-18, TGF-β, and TNF-α in aortic tissue were not a significant difference between the AAC and sham groups, but IL-1β, IL-18, TGF-β1, and TNF-α were upregulated in the AAC+MOTS-c group compared to the AAC group. Similarly, no difference in gene expression of IL-1β, IL-18, and TNF-α in heart tissue was observed between the AAC and sham groups, however, downregulated TGF-β1 levels. Conversely, IL-18 and TGF-β1 levels were approximately increased 10-fold in the AAC+MOTS-c group compared to the AAC group.

Conclusion: Our study revealed that inflammatory response genes were regulated by MOTS-c peptides. This peptide may have protective effects on cardiovascular damage progression.

Marano G, et al.(2002) Attenuation of aortic banding-induced cardiac hypertrophy by propranolol is independent of beta-adrenoceptor blockade. J Hypertens 20: 763–769 Dickhout JG, Carlisle RE, Austin RC. Interrelationship between cardiac hypertrophy, heart failure, and chronic kidney disease: endoplasmic reticulum stress as a mediator of pathogenesis. Circ Res. 2011 Mar 4;108(5):629-42. Nashine S, Kenney MC. Effects of Mitochondrial-Derived Peptides (MDPs) on Mitochondrial and Cellular Health in AMD. Cells. 2020 Apr 29;9(5):1102. Yang Y, Gao H, Zhou H, Liu Q, Qi Z, Zhang Y, Zhang J. The role of mitochondria-derived peptides in cardiovascular disease: Recent updates. Biomed Pharmacother. 2019 Sep;117:109075.

C13

Micro-dystrophin therapy rescues impaired Na currents in cardiac Purkinje fibers from dystrophin-deficient mdx mice

Janine Ebner[1], Xiufang Pan[2], Yongping Yue[2], Jessica Marksteiner[1], Xaver Koenig[1], Karlheinz Hilber[1], Dongsheng Duan[2]

[1]Department of Neurophysiology & Neuropharmacology, Center for Physiology & Pharmacology, Medical University of Vienna, Vienna, Austria, Vienna, Austria, [2]Department of Molecular Microbiology and Immunology, The University of Missouri, Columbia, MO, Columbia, United States

Cardiac arrhythmias significantly contribute to mortality in Duchenne muscular dystrophy (DMD), a disease caused by dystrophin deficiency[1]. A major source of arrhythmias in DMD patients is impaired ventricular impulse conduction, which predisposes to ventricular asynchrony and reentrant mechanisms. Using the mdx mouse model for DMD, we recently showed that lack of dystrophin causes considerable Na current loss in Purkinje fibers, cardiomyocytes specialized for electrical impulse conduction[2]. Our finding provided a mechanistic explanation for ventricular conduction defects and concomitant arrhythmias in the dystrophic heart. Systemic adeno-associated virus (AAV) delivery of micro-dystrophin (µDys) holds great promise to treat DMD and is currently in human trials[3]. Whereas animal studies of AAV µDys therapy yielded substantial structural and functional improvements in the dystrophic heart, evidence for successful correction of arrhythmia-inducing mechanisms by µDys is completely missing. The aim of the present study was to test whether AAV µDys therapy can rescue Na current loss in dystrophic Purkinje fibers.

Male mdx-Cx40$^{eGFP/+}$ mice[2] received a single tail vein injection of AAV9 µDys vector. µDys contained the N-terminal and cysteine-rich domains, hinges 1 and 4, and spectrin-like repeats 16 to 19 of human dystrophin. 12 weeks post-injection, mice were anaesthetized (2% isoflurane, inhalation) and euthanized by cervical dislocation. Thereafter, hearts were removed, and single Purkinje fibers were isolated from ventricular tissue according to our published protocol[2], whereby the Cx40$^{eGFP/+}$ background allowed for unambiguous identification of Purkinje fibers for electrophysiological studies. Na currents were recorded with the whole cell patch clamp technique, and compared with Na currents of Purkinje fibers isolated from age- and sex-matched untreated mdx-Cx40$^{eGFP/+}$ and wild-type-Cx40$^{eGFP/+}$ mice. All procedures had local approval (BMWFW-66.009/0175-WF/V/3b/2015) and conformed to the guidelines from Directive 2010/63/EU of the European Parliament on the protection of animals used for scientific purposes.

Twelve weeks after AAV µDys vector application to mdx-Cx40$^{eGFP/+}$ mice, we observed robust µDys expression in the heart. The Na current density in Purkinje fibers isolated from these hearts (-72 ± 6 pA/pF, mean ± S.E.M, 20 cells from 6 animals) was restored to the wild-type level (-74 ± 4 pA/pF, 58 cells from 8 animals; p=0.86, nested statistical analysis respecting the hierarchical data structure[4]). Impaired Na channel inactivation, represented by a moderately slowed current decay in mdx compared to wild-type fibers, was also rescued by µDys therapy.

Na channel activity in the Purkinje fiber membrane determines ventricular conduction velocity[2]. Thus, by restoring wild-type Na current properties in dystrophic Purkinje fibers, we have

corrected the molecular underpinning of impaired ventricular conduction in the dystrophic heart. Further development of this therapeutic strategy may prevent or treat fatal arrhythmias in patients with DMD.

Abbreviations: adeno-associated virus, AAV; Duchenne muscular dystrophy, DMD; micro-dystrophin, μDys

1. Duan D et al. (2021). Nat Rev Dis Prim 7, 13. 2. Ebner J et al. (2020). Am J Physiol - Hear Circ Physiol 318, H1436–H1440. 3. Duan D (2018). Mol Ther 26, 2337–2356. 4. Sikkel MB et al. (2017). Cardiovasc Res. 113, 1743–1752.

C14

SparkMaster 2: A new software for automatic analysis of calcium spark data

Jakub Tomek[1,2], Madeline Nieves-Cintron[2], Manuel Navedo[2], Christopher Ko[2], Donald Bers[2]

[1]University of Oxford, Oxford, United Kingdom, [2]UC Davis, Davis, United States

Introduction: Calcium (Ca) sparks are elementary units of subcellular Ca release in cardiomyocytes and other cells. Accordingly, Ca spark imaging is an essential tool for understanding physiology and pathophysiology of Ca handling and is used to identify new drugs targeting Ca-related cellular dysfunction (e.g., cardiac arrhythmias). The large volumes of imaging data produced during such experiments require accurate and high-throughput analysis.

Objective: To produce a new improved software tool for the analysis of Ca sparks imaged by confocal line-scan microscopy, combining high accuracy, flexibility, and user-friendliness.

Methods and Results: We created a new open-source Python-based software tool SparkMaster 2 (SM2) for the analysis of line-scan spark imaging data, with the following key strengths: 1) high accuracy at identifying Ca release events, clearly outperforming previous highly successful software SparkMaster; 2) multiple types of Ca release events can be identified using SM2: Ca sparks, waves, mini-waves, and long sparks; 3) SM2 can accurately split and analyze individual sparks within spark clusters, a capability not handled adequately by prior tools. We demonstrate the practical utility of SM2 on two case studies, investigating how Ca levels affect spontaneous Ca release, and how large-scale release events may promote release refractoriness. Broad usefulness across cell types and imaging conditions is also shown. SM2 is distributed as a stand-alone application requiring no installation. It can be controlled using a simple-to-use graphical user interface, or using Python scripting.

Conclusions: SparkMaster 2 is a new and much improved user-friendly software for accurate high-throughput analysis of line-scan Ca spark imaging data. It is free, easy to use and provides valuable built-in features to facilitate visualization, analysis and interpretation of Ca spark data. It should enhance the quality and throughput of Ca spark and wave analysis across cell types, particularly in the study of arrhythmogenic Ca release events in cardiac myocytes.

C19

S-nitrosylation of CaMKIIδ can modulate the progression of cardiac arrhythmias in isolated hearts during stress

Esther Asamudo[1], Jeffrey Erickson[2], Donald Bers[1]

[1]Department of Pharmacology, University of California, Davis, Davis, United States,
[2]Department of Physiology and HeartOtago, School of Biomedical Sciences, University of Otago, Dunedin, New Zealand

Introduction: Nitric oxide can regulate cardiac function by targeting calcium-handling protein kinases such as calcium/calmodulin-dependent protein kinase II delta (CaMKIIδ). Recent evidence has shown that during stress response, there is an increase in nitric oxide production which can activate CaMKII through *S*-nitrosylation. Chronic CaMKII activation, as a result of *S*-nitrosylation, has been implicated in the progression of arrhythmias. However, CaMKII *S*-nitrosylation can have protective or detrimental effects on cardiac function depending on the *S*-nitrosylation site that is modified. In the heart, the Cys 273 site inhibits CaMKII activation while the Cys 290 site enhances autonomous CaMKII activity. The mechanism underlying the role of CaMKII *S*-nitrosylation sites in the regulation of cardiac function during acute ischemia/reperfusion (I/R) injury has not been fully elucidated.

Aim: To determine if CaMKII S-nitrosylation site was detrimental to the heart during I/R injury.

Methods: Male mouse hearts were isolated and perfused with modified Krebs-Henseleit buffer via the Langendorff perfusion system. Hearts from wild-type C57BL/6 (WT) (n = 5) and C273S knock-in mice (C273S-KI, that lack the Cys 273 site; n = 5) were acutely exposed to 100 nM isoproterenol (ISO), a β-adrenergic receptor agonist before or after 150 μM S-nitrosoglutathione (GSNO), a nitric oxide donor for 10 min. Arrhythmias were counted per heart. For ischemia studies, WT (n = 4 – 6) and C273S-KI (n = 3) hearts were exposed to 100 nM ISO for 5 min prior to 20 min global ischemia, followed by 90 min reperfusion. Duration of arrhythmias was measured for 10 minutes post-ischemia. Data is presented as mean ± standard error of mean and ANOVA was used determine the variance in means.

Results: Treatment of isolated WT hearts with GSNO before ISO reduced arrhythmias compared to control (15.2 ± 4.2 vs 7.6 ± 2.4; $p<0.05$) while treating isolated hearts with ISO before GSNO promoted arrhythmias compared to control (38.0 ± 14.5 vs 4.6 ± 1.4; $p < 0.05$). When *S*-nitrosylation at C273 was not available in C273S-KI hearts, ISO before GSNO significantly increased arrhythmic events and GSNO before ISO had the similar effects (46.2 ± 23.2 vs 5.5 ± 2.9; 46.5 ± 8.9 vs 4.0 ± 1.7; $p<0.05$). The ischemic WT hearts and C273S-KI hearts had similar % LVDP recovery after ISO treatment. In addition, we did not detect a difference in the duration of arrhythmic events early during reperfusion in WT and C273S-KI hearts before (175.0 ± 41.3 vs 196.7 ± 38.4 secs) and after (277.5 ± 96.0 vs 336.7 ± 132.5 secs) treatment with ISO.

Conclusion: Our findings suggest that CaMKII *S*-nitrosylation at Cys 273 may provide some protection against ISO-induced arrhythmias. Our preliminary ischemia experiments showed no significant benefit of Cys 273 presence on post-ischemic LVDP recovery or early arrhythmias, without prior GSNO treatment. We are still testing the hypothesis that pre-treatment with GSNO

before ischemia will provide protection in WT, but not in the C273S knock-in mouse. If that hypothesis is supported, *S*-nitrosylation of CaMKIIδ at Cvs 273 may be a more generally protective event under β-adrenergic and ischemia-reperfusion stress.

C20

Targeting Runx1 prevents regional heterogeneity of impaired calcium handling post-MI

Eilidh MacDonald[1], Holly Watson[1], Tamara Martin[1], Stuart Nicklin[1], Ewan Cameron[1], Christopher Loughrey[1]

[1]University of Glasgow, Glasgow, United Kingdom

Following myocardial infarction (MI), dead cardiomyocytes are replaced by collagenous scar and result in a heterogenous transition zone between the scar and healthy myocardium. The region of myocardium bordering an infarct (border zone, BZ) undergoes many transcriptional changes, some of which may drive adverse remodelling. Master regulator transcription factor *Runx1* is increased in the BZ as early as 1 day post-MI. Previously, we have shown that cardiomyocyte-specific *Runx1* deficient (*Runx1*$^{\Delta/\Delta}$) mice demonstrate remarkably preserved contractility 1 day post-MI and that *Runx*1 modulates cardiac sarcoplasmic reticulum (SR) calcium uptake and contractile function (McCarroll et al. 2018). Ventricular arrhythmias and sudden cardiac death are major complications over the days and weeks following MI, the BZ region being most vulnerable site for arrhythmogenesis. (Qin et al. 1996). As such, we hypothesised that changes in *Runx*1 may contribute to arrhythmogenicity in the BZ region post-MI.

It is well understood that both heterogenous tissue electrophysiology and impaired calcium handling can result in an increased propensity for arrhythmia (Smaill et al. 2013). Thus, calcium measurements were performed on BZ and remote zone (RZ) cardiomyocytes loaded with a calcium-sensitive fluorophore (5.0 µmol/L Fura-4F AM, Invitrogen) from *Runx*1$^{\Delta/\Delta}$ and flox control (*Runx*1$^{fl/fl}$) mice.

Overall, we found that at 1-day post-MI, BZ cardiomyocytes from *Runx*1$^{fl/fl}$ mice had impaired calcium handling compared to RZ cardiomyocytes, whereas there were no regional differences in *Runx1*$^{\Delta/\Delta}$ mice. Specifically, in BZ cardiomyocytes, calcium transient peak was 64% of the RZ peak, whereas in *Runx1*$^{\Delta/\Delta}$ hearts, calcium transient peak was not different in the BZ compared to the RZ. Calcium transient amplitude in the BZ was 47% of that observed in RZ cardiomyocytes *Runx*1$^{fl/fl}$ mice, whereas it was preserved in *Runx1*$^{\Delta/\Delta}$ hearts. This pattern was also consistent for caffeine-induced calcium transient amplitude, representing SR calcium content, was 71% of that observed in RZ cardiomyocytes in *Runx*1$^{fl/fl}$ mice but again not different regionally in *Runx1*$^{\Delta/\Delta}$ hearts and SERCA activity, quantified by the rate constant of decay of the caffeine-induced calcium transient, which was 48% of RZ cardiomyocytes in the BZ of *Runx*1$^{fl/fl}$ mice but not different between Runx1$^{\Delta/\Delta}$ BZ and RZ cardiomyocytes.

Further, in ventricular cardiomyocytes isolated from C57BL/6 mice and incubated with *Runx*1 small molecule inhibitor Ro5-3335 or with vehicle control DMSO, we utilised a burst pacing protocol followed by a two-minute period of rest and measured spontaneous calcium events as a measure of arrhythmogenicity. We found that cells treated with Ro5-335 had significantly fewer spontaneous events in the rest period compared cells incubated in DMSO (0.5 ± 0.02 *vs*. 26 ± 8, $p = 0.017$, $n = 9$). Overall, these results demonstrate the potential mechanistic contribution of Runx1 to arrhythmogenicity in the BZ post-MI.

McCarroll CS, He W, Foote K, et al (2018) Runx1 deficiency protects against adverse cardiac remodeling after myocardial infarction. Circulation 137:57–70. https://doi.org/10.1161/CIRCULATIONAHA.117.028911 Qin D, Zhang ZH, Caref EB, et al (1996) Cellular and ionic basis of arrhythmias in postinfarction remodeled ventricular myocardium. Circ Res 79:461–73. https://doi.org/10.1161/01.res.79.3.461 Smaill BH, Zhao J, Trew ML (2013) Three-dimensional impulse propagation in myocardium. Circ Res 112:834–848. https://doi.org/10.1161/CIRCRESAHA.111.300157

C21

The entrainment of action potential duration and contractile amplitude by recapitulation of respiratory sinus arrhythmia in isolated cardiac myocytes requires a functioning sarcoplasmic reticulum

Alexander Carpenter[1], Andrew Butler[2], Laura Pannell[1], Julian Paton[3], Jules Hancox[1], Andrew James[1]

[1]School of Physiology, Pharmacology & Neuroscience, University of Bristol, Bristol, United Kingdom, [2]School of Physiology, Pharmacology & Neuroscience, University of Bristol,, Bristol, United Kingdom, [3]The Heart Research Centre, University of Auckland, Auckland, New Zealand

Respiratory sinus arrhythmia (RSA) is the oscillation of heart rate in phase with ventilation and represents the high frequency component of heart rate variability. RSA is prevalent in the young and the endurance-trained and its loss in heart failure is considered a prognostic indicator for sudden death. The recapitulation of RSA improves cardiac function in animal models of heart failure (O'Callaghan *et al.*, 2020; Shanks *et al.*, 2022). However, the precise mechanisms by which RSA affects cardiac function are unknown. We have previously shown that recapitulation of RSA through oscillatory pacing (OP), in which cycle length (CL) was set to 20% below and 20% above the average basic CL in a 2-short, 2-long stimulus train, entrained action potential duration (APD), Ca^{2+} transient amplitude (CaT) and sarcomere shortening and reduced the incidence of alternans in comparison to pacing at constant CL in guinea pig isolated ventricular myocytes (Carpenter *et al.*, 2021; Carpenter *et al.*, 2022). The OP entrainment of CaT and sarcomere shortening persisted in voltage clamp experiments with fixed APD (i.e. AP clamp), suggesting that APD is not an essential component of entrainment. Here, we examine the hypothesis that OP in isolated ventricular myocytes affects the stimulus-interval dependence of APD and sarcomere shortening through mechanisms involving the sarcoplasmic reticulum (SR). Animal procedures were approved by the University of Bristol Animal Welfare and Ethics Review Board and conducted according to UK legislation. Hearts were excised from adult male guinea pigs under general anaesthesia (140 mg/kg bodyweight euthatal, i.p.) and left ventricular myocytes isolated following enzymatic digestion. Isolated myocytes were superfused with Tyrode's solution at 37 °C for perforated patch whole-cell current clamp recording and action potentials and sarcomere length measured simultaneously. Sample sizes are presented as *n* (number of cells) from *N* (number of animals) and nested hierarchical analysis applied using a generalized linear mixed model (SPSS, IBM). The limit of statistical confidence was $P<0.05$. Using a three-step $S_1S_2S_3$ protocol to examine the dependence of APD and sarcomere shortening on both preceding (CL_{n-1}) and anteceding (CL_{n-2}) stimulus intervals, both APD and sarcomere shortening were found to depend directly on the preceding cycle length (CL_{n-1}, $P<0.001$). In contrast, sarcomere shortening depended *inversely* on the anteceding CL (CL_{n-2}, $P<0.001$), while APD_{90} did not depend significantly on CL_{n-2} ($n/N = 24/4$). This is consistent with the entrainment by OP, the effect of CL_{n-1} on sarcomere shortening being akin to post-extrasystolic potentiation (Yue *et al.*, 1985). Following treatment of the cells with caffeine (50 μM) to sensitise ryanodine receptors, both APD and sarcomere shortening in response to the CL_{n-1} stimulus were markedly suppressed, and the inverse dependence of sarcomere shortening on anteceding CL_{n-2} was lost ($P<0.001$, $n/N = 6/3$). These data are consistent with an obligatory role for the SR in the entrainment of APD, CaT and sarcomere shortening and the suppression of alternans by the recapitulation of RSA. Further work is required on the effects of OP in intact hearts to determine the potential for a protective effect of RSA recapitulation against ventricular tachyarrhythmias.

Carpenter A, Butler A, Paton JFR, Hancox JC & James AF. (2021). Cycle length dependence of electrical and mechanical alternans in guinea pig ventricular myocytes. In Physiology 2021, pp. PC002. Physiological Society, online. https://www.physoc.org/abstracts/cycle-length-dependence-of-electrical-and-mechanical-alternans-in-guinea-pig-ventricular-myocytes/ Carpenter A, Butler AS, Pannell LMK, Paton JFR, Hancox JC & James AF. (2022). Recapitulation of heart rate variability suppresses alternans in guinea pig ventricular myocytes. In Europhysiology 2022, pp. A08-22. Scandinavian Physiological Society, Copenhagen. https://europhysiology2022.org/scientific-programme/ O'Callaghan EL, Lataro RM, Roloff EL, Chauhan AS, Salgado HC, Duncan E, Nogaret A & Paton JFR. (2020). Enhancing respiratory sinus arrhythmia increases cardiac output in rats with left ventricular dysfunction. J Physiol (Lond) 598, 455-471. doi: 10.1113/jp277293 Shanks J, Abukar Y, Lever NA, Pachen M, LeGrice IJ, Crossman DJ, Nogaret A, Paton JFR & Ramchandra R. (2022). Reverse re-modelling chronic heart failure by reinstating heart rate variability. Bas Res Cardiol 117, 4. doi: 10.1007/s00395-022-00911-0 Yue DT, Burkhoff D, Franz MR, Hunter WC & Sagawa K. (1985). Postextrasystolic potentiation of the isolated canine left ventricle. Relationship to mechanical restitution. Circ Res 56, 340-350. doi: 10.1161/01.RES.56.3.340

C22

Interactions between MARCKS, cav1.2 and PIP2 in cardiac myocytes, a potential novel pathway in heart failure and arrhythmogenesis

Yousif A Shamsaldeen[1,2], Anthony P Albert[1]

[1]Molecular & Clinical Sciences Research Institute, St. George's, University of London, London, United Kingdom, [2]School of Applied Sciences, University of Brighton, Brighton, United Kingdom

Introduction:

Cardiovascular disease (CVD) is a leading public health problem in the UK, with over 7 million people affected and at a cost of more than 150,000 deaths and £10 billion annually. Such a major cause of morbidity, mortality and economic burden reveals a huge medical need for novel therapeutic targets to treat CVD. It is well established that stimulation of CaV1.2 voltage-gated Ca^{2+} channels (VGCCs) plays a fundamental role in cardiac cell function, regulating both rate and rhythm and contractility of the heartbeat. Therefore, understanding novel regulatory mechanisms of CaV1.2 VGCCs may reveal new targets to treat CVD such as heart failure and arrhythmogenesis. We recently showed that myristoylated alanine-rich C kinase substrate (MARCKS) acts as phosphatidylinositol 4,5-bisphosphate (PIP_2) buffer to regulate the activity of CaV1.2 VGGCs and vasoconstriction of mesenteric arteries (Jahan et al. 2020).

Aim: In the present study, we have investigated whether similar mechanisms are present in cardiomyocytes.

Methods:

All animal procedures were carried out in accordance with guidelines laid down by St George's, University of London Animal Welfare Committee and conform with the principles and regulations described by the Service Project Licence: 70/8512 Freshly isolated heart lysates and cardiomyocytes from hearts of male Wistar rats were studied through a wide range of techniques including western blotting, immunocytochemistry, proximity ligation assay (PLA), and whole-cell patch clamp electrophysiology.

Results:

In western blot studies, expression levels of MARCKS, CaV1.2, and PIP_2 were similar in right atrium, right ventricle, left atrium, and left ventricle (n= 7, $p>0.05$, one-way ANOVA). When heart samples were incubated with wortmannin (20 μM), PIP_2 levels were significantly supressed in all heart chambers ($P<0.0001$, one-way ANOVA). The functionality of MARCKS on VGCCs was then investigated using the MARCK activator, MANS peptide (100 μM), which significantly increased whole-cell Ba^{2+} currents from 3.19 ± 0.34 pA/pF to 6.05 ± 0.43 pA/pF at 0 mV (n= 7, $p<0.001$, t-test). This effect of MANS peptide was abolished when cells were preincubated with wortmannin (20 μM). Immunocytochemistry and PLA studies demonstrated that MARCKS and PIP_2 colocalise significantly at resting condition. However, upon stimulation with MANS peptide, this colocalization of MARCKS and PIP_2 was reduced and CaV1.2 was shown to colocalise with PIP_2 (n= 6, $P<0.0001$, t-test).

Conclusion:

These preliminary findings reveal the expression and interaction between MARCKS, CaV1.2 and PIP_2 in cardiomyocytes, which likely controls cardiomyocytes calcium homeostasis. These molecular complexes may play an essential role in regulating cardiac function, and may be altered in cardiac dysfunction, thus providing a novel target for treating CVD.

Jahan, K. S., et al. (2020). MARCKS mediates vascular contractility through regulating interactions between voltage-gated Ca2+ channels and PIP2. Vascular Pharmacology 132: 106776.

C23

Characterising a novel cardiac phenotype in Niemann-Pick Disease Type C

Qianqian Song[1], Rebecca Capel[1], Thamali Ayagama[2], David Priestman[1], Reuben Bush[1], Ming Lei[1], Frances Platt[1], Rebecca Burton[1]

[1]Department of Pharmacology, University of Oxford, Oxford, United Kingdom, [2]Department of Physiology, Anatomy and Genetic, University of Oxford, Oxford, United Kingdom

Introduction: Niemann-Pick disease Type C (NPC) is an autosomal recessive disease that is caused by mutations in two genes, *NPC1* or *NPC2* that encode lysosomal proteins. Mutations in either gene result in the accumulation of cholesterol, sphingomyelin and glycosphingolipids in lysosomes[1]. The principal clinical manifestations include hepatosplenomegaly, ataxia, seizures and neurodegeneration. No in-depth studies have been performed on cardiac function in these patients. Recent studies have shown that Ca^{2+} released from acidic stores such as lysosomes can take a part in cytosolic Ca^{2+} transients, enhancing contraction amplitude and speed[2]. NPC cells have reduced levels of lysosomal Ca^{2+}[3], thus, it is possible that altered Ca^{2+} signalling in cardiomyocytes can affect the lysosome mediated Ca^{2+} signalling cascade and may be potentially arrhythmogenic.

Aims: To characterise the NPC mouse heart both structurally and at the molecular level, and to investigate its susceptibility to arrhythmia.

Methods: All experiments complied with the United Kingdom Home Office Guide on the Operation of Animal (Scientific Procedures) Act of 1986. Wild-type (WT) and *Npc1*$^{-/-}$ mice were bred from heterozygous BALBc/cNctr- Npc1^{m1n}/J. Masson's trichrome and picrosirius red staining was performed on heart sections to assess the level of fibrosis and further validated by western blotting of the fibrosis marker collagen I and vimentin. *Npc1*$^{-/-}$ heart electrophysiology (ECG) was performed on a Langendorff perfusion system using electrical (burst pacing) and pharmacological (50nM isoprenaline) protocols. We also performed a transcriptomic analysis on *Npc1*$^{-/-}$ hearts at 3, 7 and 9 weeks of age to investigate the molecular mechanism involved in *Npc1*$^{-/-}$ cardiac pathophysiology development at the transcriptional level.

Result: Histological staining revealed significantly increased fibrosis in *Npc1*$^{-/-}$ heart sections at 7 weeks of age (WT 17.1%±0.3 vs NPC 19.4%±0.28, $p<0.0001$, n=3). Western blot for collagen I and vimentin supported the histology results, with increased levels of collagen I and vimentin in NPC tissue ($p=0.0261$ or 0.0435 respectively, n=6). Compared to WT, *Npc1*$^{-/-}$ hearts had significantly pro-longed QT interval for 11.7 ms ($p=0.0029$, n=7), suggesting a change in ion channel function. Also, *Npc1*$^{-/-}$ hearts presented ECG abnormalities including arrhythmias under pharmacological stress. Transcriptomic analysis found 3240, 2190 and 5300 differential expressed genes (DEGs) comparing hearts at 3, 7 and 9 weeks of age ($p<0.05$, n=5). Several significantly altered cellular pathways were identified including immune/inflammation response, lysosome, calcium signalling, arrhythmogenic right ventricular cardiomyopathy, and adrenergic signalling, which support our hypothesise that *Npc1*$^{-/-}$heart is more susceptible to arrhythmia.

Conclusion: Our studies highlight in *Npc1-/-* hearts fibrotic remodelling, inflammation and ion signalling alterations. We provide the first evidence that NPC hearts have a higher tendency to

display structural and functional disturbances including arrhythmias as a consequence of lysosomal Ca^{2+} signalling defects in the heart.

1. Vanier, M. T. (2010). Niemann-Pick disease type C. Vanier Orphanet Journal of Rare Diseases (Vol. 5). http://www.ojrd.com/content/5/1/16 2. Capel RA, Bolton EL, Lin WK, Aston D, Wang Y, Liu W, et al. Two-pore Channels (TPC2s) and Nicotinic Acid Adenine Dinucleotide Phosphate (NAADP) at Lysosomal-Sarcoplasmic Reticular Junctions Contribute to Acute and Chronic β-Adrenoceptor Signaling in the Heart. Journal of Biological Chemistry. 2015;290(50):30087–98. 3. Lloyd-Evans, E., Morgan, A. J., He, X., Smith, D. A., Elliot-Smith, E., Sillence, D. J., Churchill, G. C., Schuchman, E. H., Galione, A., Platt, F. M. (2008). Niemann-Pick disease type C1 is a sphingosine storage disease that causes deregulation of lysosomal calcium. Nature Medicine, 14 (11), 1247–1255. DOI:10.1038/nm.1876

C24

Alpha-synuclein mediated molecular remodeling of the myocardium and stellate ganglia in the aged Parkinson's disease animal model.

Bonn Lee[1], Charlotte Edling[1], Shiraz Ahmad[1], Fiona LeBeau[2], Kamalan Jeevaratnam[1]

[1]School of Veterinary Medicine, Faculty of Health and Medical Sciences, University of Surrey, Guildford, United Kingdom, [2]Biosciences Institute, Faculty of Medical Sciences, Newcastle University, Newcastle upon Tyne, United Kingdom

Ion channels play a vital role in cardiac electrophysiology by modulating the inotropic and chronotropic action and the cardiac electrophysiology in turn is modulated by the autonomic nervous system (ANS). In recent years studies have shown a correlation between cardiac disease and Parkinson's disease (PD) which features the degeneration of ANS. However, the mechanism causing the evident cardiac denervation in PD remains unclear. A30P missense mutation of alpha-synuclein is a risk factor of familial PD, and alpha-synucleinopathy is the hallmark of PD. We aimed to investigate the link between alpha-synucleinopathy and cardiac ion channel remodelling with the aid of the A30P transgenic PD mice model.

For our studies, eight groups of wildtypes and A30P transgenic mice, young and old, male and female were investigated (n = 4 each group, total 32 samples). We performed RNA-sequencing of the heart and stellate ganglia. Immunohistochemistry was conducted to investigate the mutant protein expression. Our data revealed that the A30P transgenic mice present with mutant alpha-synuclein in the heart and stellate ganglia and with up-regulated pro/anti-inflammatory markers on the mRNA level. Additionally, the mRNA expression of cardiac ion channels was significantly changed.

Our results indicate that mutation of alpha-synuclein can result in alterations in cardiac and sympathetic ganglionic tissue including cardiac ion channel remodelling and an inflammatory reaction following alpha-synucleinopathy development. To investigate further we aim to study the phenotype of the electrophysiological modifications. In conclusion, here we demonstrate a transcriptional link between the ANS and cardiac electrophysiology which can help identify and explain the increased risk of cardiac disease in PD patients.

Kahle, P. J. et al. (2000), J. Neurosci, 20(17), 6365-6373. Javanshiri et al. (2022), J Parkinsons Dis, 12, 1125-1131.

C25

Chronic hypoxia and mitochondrial inhibition upregulate noradrenaline transporter function in the rat left atrium

James Saleeb-Mousa[1], Andrew Coney[1], Shadman Ahmed[1], Manish Kalla[1], Keith Brain[1], Andrew Holmes[1]

[1]School of Biomedical Sciences, Institute of Clinical Sciences, University of Birmingham, Birmingham, United Kingdom

Cardiac remodelling in AF is associated with functional heterogeneity within the atria, giving rise to ectopic and re-entrant activity. Significant atrial remodelling is seen following exposure to chronic hypoxia (CH). This is likely attributable, in part, to dysregulated cardiac autonomic control, of which the noradrenaline transporter (NAT) is a key regulator. Therefore, we investigated regional differences in left atrial NAT function in normoxic (N) and CH-exposed rats (FiO_2=0.12, 9-10 days). Regional innervation density was also compared in N and CH within the left atrium. Since CH is associated with adaptive changes in metabolic function, we also investigated the effect of mitochondrial inhibition on NAT dynamics.

To investigate single-terminal NAT dynamics, we employed a recently developed confocal fluorescence technique using the NAT-specific neurotransmitter uptake assay (NTUA; Molecular Devices, USA) (Cao et al. 2020). Experiments and procedures were performed in accordance with the UK Animals (Scientific Procedures) Act 1986. Hearts were excised from male Wistar rats (200-300g) under non-recovery terminal inhalation isoflurane (3-5% in O_2, flow rate 1.5L min^{-1}) with death confirmed by cervical dislocation. Ventricles were dissected free and atria were transferred to a superfusion chamber. Tissues were dissected into left atrial appendage (LAA), left atrial posterior wall (LAPW) and pulmonary veins (PV). Sections were pinned flat and transferred to a confocal microscope. Immediately after NTUA loading, image stacks were captured over 15 minutes to allow calculation of single-terminal NTUA uptake (n=6 terminals per region). Imaging was performed for N tissues (n=5 rats), CH tissues (n=3-5 rats), and in an additional subset of normoxic rats where sodium azide (10μM), a complex IV inhibitor, was added to the NTUA solution (n=4-5 rats). Additional images were acquired at low magnification to allow calculation of innervation density. Two-way ANOVA was performed for statistical analysis with Bonferroni testing for multiple comparisons. Values are expressed as mean ±SEM.

CH rats demonstrated a relative right ventricular hypertrophy compared to N rats ($p<0.0001$). Analysis of uptake traces in all tissues revealed a two-phase association characterized by an initial 6-minute linear uptake followed by a plateau phase. Maximum fluorescence (F_{Max}) and linear uptake gradients (F_L) were not significantly different between atrial regions in N tissues ($p>0.05$). In CH animals, LAA terminals showed increased F_{Max} ($p=0.004$) and F_L ($p=0.021$) compared to N. NAT dynamics the LAPW and PV were unchanged in CH ($p>0.05$). CH was also associated with a generalised increase in atrial innervation density, independent of region ($p=0.034$). Sodium azide exposure was also associated with an increase in F_L in the LAA ($p=0.030$), as well as an increase in F_{Max} in the LAPW ($p<0.001$).

Our data demonstrate functional variability in the left atrial response to CH and mitochondrial inhibition. Further investigation is required to determine the role of hypoxic dysregulation of the NAT in arrhythmogenesis.

1. Cao L et al. (2020). Auton Neurosci 223, 102611.

C26

Examining the influence of intact heart activation time on the action potential duration of ventricular cardiomyocytes

Rebecca Gilchrist[1], John McClure[1], Francis Burton[1], Godfrey Smith[1], Rachel Myles[1]

[1]School of Cardiovascular and Metabolic Health, University of Glasgow, Glasgow, United Kingdom

Introduction: Spatial heterogeneity of action potential duration (APD) is key to arrhythmia generation in the ventricle[1,2]. Our previous intact heart studies have suggested that earlier-activating regions of the ventricle have longer APD at baseline and show exaggerated response to I_{Kr} blockade, thereby contributing to increased spatial APD heterogeneity. However, it is unclear whether these effects result from differences in intrinsic cardiomyocyte properties between earlier and later activating ventricular regions, or from electrotonic coupling between neighbouring cardiomyocytes and Purkinje cells[3]. A series of combined optical mapping and cardiomyocyte isolation experiments were, therefore, performed to compare differences in intrinsic APD between cardiomyocytes isolated from earlier and later activating ventricular regions.

Objective: To determine whether the intact heart activation sequence influences the APD of ventricular cardiomyocytes.

Methods: All procedures involving animals were carried out in accordance with the UK Animals (Scientific Procedures) Act 1986 under project licence PP5254544. Male New Zealand White rabbit hearts (N=6) were Langendorff-perfused with oxygenated Tyrode's solution (37±0.5°C) containing FluoVolt and blebbistatin. Optical signals reflecting transmembrane voltage were recorded from the anterior epicardial surface of the hearts, then activation time maps constructed. Cardiomyocytes were then enzymatically isolated from five regions of the left and right ventricles with distinct activation times. Isolated cardiomyocytes were loaded with FluoVolt, then fluorescence traces reflecting transmembrane voltage were recorded from single cardiomyocytes by an investigator blinded to the origin of each cardiomyocyte group. The effect of activation time on APD_{90} in the intact heart was quantified for each heart using simple linear regression analysis. The effect of intact heart activation time on isolated cardiomyocyte APD_{90} was assessed using a linear mixed-effects model with unstructured covariance matrix. 'Animal' was included as a grouping variable with random intercept, and 'activation time' and 'ventricle' were included as fixed effects.

Results: A consistent inverse relationship between activation time and APD_{90} was observed in the intact heart during sinus rhythm (mean slope: -0.865±0.132, mean r^2:0.602±0.084; N=6 hearts). Linear mixed-effects analysis revealed significant evidence for a main effect of intact heart activation time on APD_{90} of isolated cardiomyocytes (slope estimate: -0.814, 95% CI: -1.327 to -0.300, P=0.0020). There was also significant evidence for a main effect of ventricle on APD_{90}, with shorter APD_{90} detected among RV myocytes than LV myocytes (slope estimate: -17.611, 95% CI: -22.011 to -13.211, P<0.0001).

Conclusion: These findings suggest that the intact heart activation sequence may influence APD at both the intact heart and cardiomyocyte level, such that cardiomyocytes located within earlier activating regions of the ventricle have longer APD.

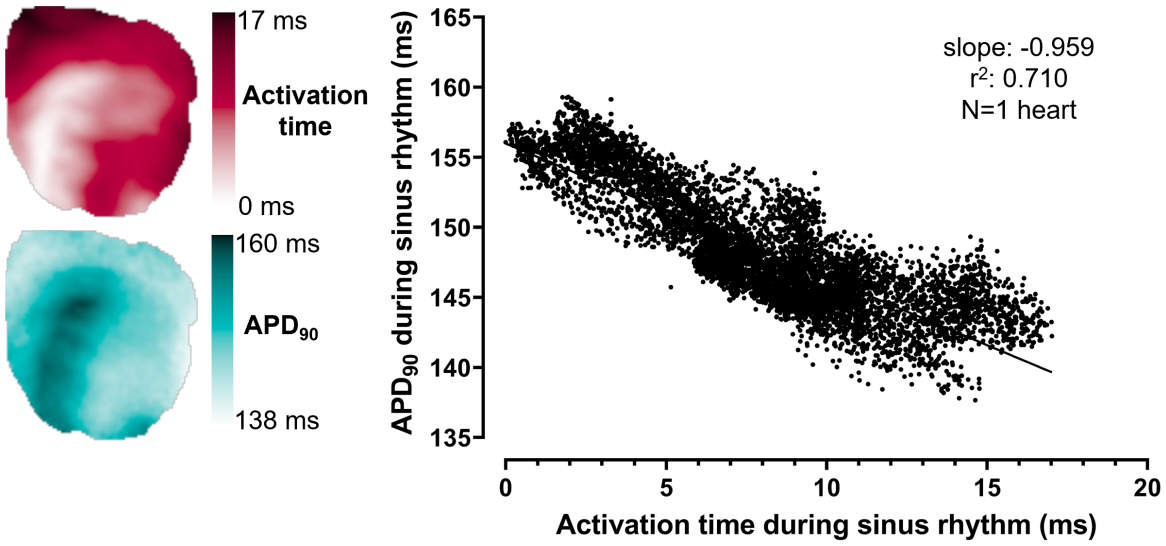

Figure 1. Relationship between activation time and APD_{90} in the intact heart during sinus rhythm. Typical maps showing the patterns of activation time and APD_{90} across the epicardial surface of a single heart. The results of the linear regression analysis of activation time vs APD_{90} for the same heart are shown (N=1, n=7155 pixels).

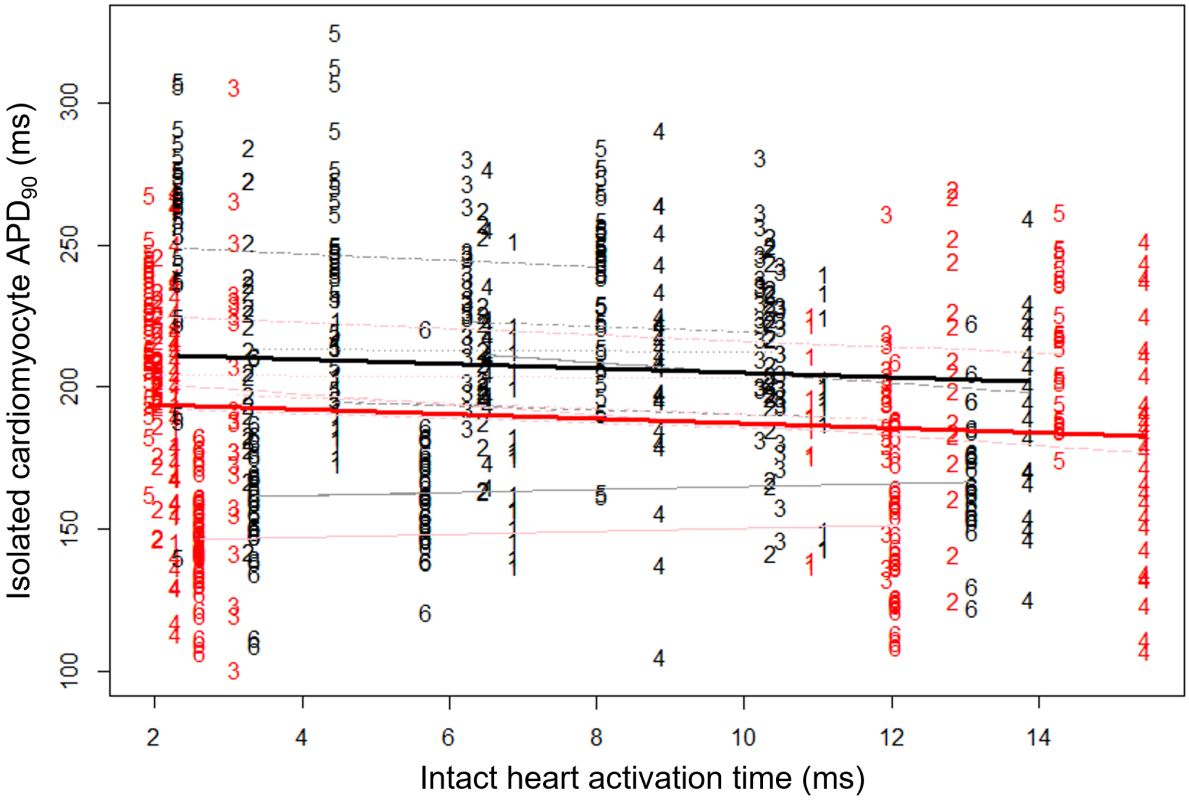

Figure 2. Relationship between intact heart activation time and isolated cardiomyocyte APD_{90}. Right ventricular myocytes are shown in red and left ventricular myocytes are shown in black. Cardiomyocytes isolated from the same animal are shown by the same number (N=6 hearts, n=761 cardiomyocytes).

1. Maruyama M et al. (2011). Circ Arrhythm Electrophysiol. 4(1):103-11. 2. Dunnink A et al. (2017). Europace. 19(5):858–865. 3. Walton RD et al. (2014). Cardiovasc Res. 103(4):629-40.

C27

Long QT syndrome-associated calmodulin variants D130V and E141K alter RyR2 and Cav1.2 calcium channel activity

Kirsty Wadmore[1], Caroline Dart[1], Nordine Helassa[1]

[1]Department of Biochemistry, Cell and Systems Biology, Institute of Systems, Molecular and Integrative Biology, Faculty of Health and Life Sciences, University of Liverpool, Liverpool L69 3BX, UK, Liverpool, United Kingdom, [2]Department of Biochemistry, Cell and Systems Biology, Institute of Systems, Molecular and Integrative Biology, Faculty of Health and Life Sciences, University of Liverpool, Liverpool L69 3BX, UK, Liverpool, United Kingdom

Introduction

Approximately 1:2000 births are affected by the life-threatening cardiac arrhythmia long QT syndrome (LQTS). In recent years, there has been an increasing link between LQTS and mutations in the protein calmodulin (CaM), a calcium (Ca^{2+}) sensing protein. However, the causative mechanisms behind irregular heartbeats from these CaM variants remains elusive. CaM primarily regulates the activity of a diverse range of proteins, including the Ca^{2+} channels involved in cardiac muscle contraction: RyR2 and $Ca_v1.2$. The aim of this project is to investigate the consequences of LQTS-associated mutations D130V and E141K on CaM's structure and function, to apprehend how these variants lead to the phenotype seen in LQTS patients.

Methods

Circular dichroism was used to determine thermostability and secondary structure content of CaM variants. Isothermal titration colorimetry (ITC) was utilised to investigate the binding parameters of CaM variants for RyR2 and $Ca_v1.2$ (IQ and NSCaTE domains). Functional characterisation of the CaM variants on Ca^{2+} ion-channel activity, was investigated using Ca^{2+} imaging (RyR2) and whole-cell patch clamp electrophysiology ($Ca_v1.2$).

Results

Thermostability of the LQTS-associated variants D130V and E141K, was not altered in comparison to CaM-WT. a-helical content was significantly reduced to approximately 40% in the CaM variants, compared to 64% in CaM-WT. We demonstrate that CaM-WT binds to $RyR2_{3581-3610}$ both in the absence ($K_{d\ (apo)}$ = 5.6 ± 0.7 mM) and presence of Ca^{2+} ($K_{d\ (calcium)}$ = 125 ± 2 nM). Apo-CaM D130V, interestingly, did not bind to $RyR2_{3581-3610}$. For both variants, Ca^{2+}/CaM binding to $RyR2_{3581-3610}$ was reduced (up to 3-fold for E141K). We show that LQTS-associated variants altered the kinetic parameters of RyR2-mediated Ca^{2+} oscillations, including frequency and duration, using Ca^{2+} imaging. The K_d of Ca^{2+}/CaM for $Ca_v1.2$ binding domains was 101 ± 7 nM and 1.2 ± 0.1 mM for $Ca_v1.2$-$IQ_{1665-1685}$ and $Ca_v1.2$-$NSCaTE_{48-68}$, respectively. Affinity to $Ca_v1.2$-$IQ_{1665-1685}$and $Ca_v1.2$-$NSCaTE_{48-68}$ was reduced up to 3-fold and 2-fold respectively for the LQTS-CaM variants. Using HEK-$Ca_v1.2$ cells and patch-clamp electrophysiology, we demonstrated an increase in $Ca_v1.2$ current density at particular test potentials and significantly reduced Ca^{2+}-dependent inactivation (up to 7-fold), compared to CaM-WT.

Conclusions

These data help establish that the secondary structure of CaM is altered by these LQTS-associated variants, as well as CaMs ability to interact with and modulate cardiac muscle contraction relevant ion channels (RyR2 and $Ca_v1.2$). Prolongation of the action potential is a key feature of LQTS and would be expected due to the defects seen in RyR2 and $Ca_v1.2$ inactivation.

Acknowledgements

This work was supported by British Heart Foundation (FS/17/56/32925, FS/EXT/22/35014 to N.H.; FS/PhD/20/29025 to N.H. and K.W.) and BBSRC (BB/V002767/1 to C.D.).

C28

Long QT syndrome-associated mutations alter Calmodulin secondary protein structure and interaction with the L-type-voltage-gated Ca2+ channel, Cav1.2.

Rachael Morris[1], Caroline Dart[1], Nordine Helassa[1]

[1]Department of Biochemistry, Cell and Systems Biology, Institute of Systems, Molecular and Integrative Biology, Faculty of Health and Life Sciences, University of Liverpool, Liverpool, United Kingdom

Long QT syndrome (LQTS) is an inherited and often life-threating cardiac disorder characterized by abnormal prolongation of the QT interval on an electrocardiogram (ECG). Affecting approximately 1 in 2000 individuals, LQTS-diagnosed patients are at a greater risk of developing fatal arrhythmic symptoms, typically resulting in cardiac arrest and sudden cardiac death (SCD). Multiple genetic variations in the highly conserved calcium (Ca^{2+}) sensing protein Calmodulin (CaM) have recently been identified in human patients exhibiting LQTS phenotypes, highlighting a key role of CaM in the molecular causation of LQTS. CaM is a ubiquitous intracellular protein responsible for regulating the activity of several ion channels involved in cardiac excitation-contraction coupling and cardiac muscle contraction. However, the mechanistic aetiology of CaM-associated LQTS remains unclear and is still under investigation. One of the major cardiac ion channels CaM modulates is the L-type-voltage-gated Ca^{2+} channel, Cav1.2 which contributes to cellular depolarisation and ventricular myocyte contraction. CaM binding domains have been identified at the N-terminus (NSCaTE) and C-terminus (IQ domain) of Cav1.2, allowing for the modulation/regulation of the ion channel. Small synthetic peptides containing CaM recognition sequences were used for the characterisation of CaM-target interactions. The binding parameters of CaM with each Cav1.2 peptides in Ca2+-free (5 mM EGTA) and Ca^{2+}-bound (5 mM $CaCl_2$) conditions were determined using isothermal titration calorimetry (ITC). Secondary protein structure and thermostability details of CaM variants were determined by circular dichroism (CD), whilst proteolytic stability was determined using SDS-PAGE and densitometry analysis. We showed by using ITC that CaM binds to Cav1.2-NSCaTE and Cav1.2-IQ in a Ca^{2+}-dependent manner. CaM has a nM range binding affinity for the Cav1.2-IQ domain and a μM range for Cav1.2-NSCaTE (K_d = 2.0 ± 0.19 μM). The binding parameters of the LQTS-associated variants are significantly altered, with a reduction in affinity of up to 3-fold for Cav1.2-NSCaTE, when compared to wild-type. Using CD, we revealed that the missense mutations caused by single amino acid substitutions caused significant changes in the secondary structure content, thermostability and susceptibility to protease digestion for both CaM variants. We present novel data showing that mutations within the highly conserved calcium co-ordinating domains of CaM perturb protein structure and interaction with Cav1.2, resulting in aberrated Cav1.2/CaM complex formation. Here we are beginning to develop a mechanistic insight into the structure-function relationship of CaM-associated LQTS variants and its role in Ca^{2+} signalling dysfunction and arrhythmogenesis.

C29

Resistance to inhibitors of cholinesterase 8b (Ric-8b) are key to preserving contractile function in the murine adult heart.

Elena Tsisanova[1], Muriel Nobles[2], Sonia Sebastian[3], Keat-Eng Ng[4], Alison Thomas[5], Patricia Munroe[6], Andrew Tinker[1]

[1]Department of Clinical Pharmacology and Precision Medicine, William Harvey Research Institute, Barts and The London School of Medicine and Dentistry, Queen Mary University of London, London, United Kingdom, [2]Department of Clinical Pharmacology and Precision Medicine, William Harvey Research Institute, Barts and The London School of Medicine and Dentistry, Queen Mary University of London, London, United Kingdom, [3]Department of Clinical Pharmacology and Precision Medicine, William Harvey Research Institute, Barts and The London School of Medicine and Dentistry, Queen Mary University of London, London, United Kingdom, [4]Department of Clinical Pharmacology and Precision Medicine, William Harvey Research Institute, Barts and The London School of Medicine and Dentistry, Queen Mary University of London, London, United Kingdom, [5]Department of Clinical Pharmacology and Precision Medicine, William Harvey Research Institute, Barts and The London School of Medicine and Dentistry, Queen Mary University of London, London, United Kingdom, [6]Department of Clinical Pharmacology and Precision Medicine, William Harvey Research Institute, Barts and The London School of Medicine and Dentistry, Queen Mary University of London, London, United Kingdom

Resistance to inhibitors of cholinesterase are involved in modulating G-protein function but little is known of their potential physiological importance in the heart. In the present study, we have assessed the role of resistance to inhibitors of cholinesterase 8b (Ric-8b) in determining cardiac contractile function. We developed a novel murine model in which it was possible to conditionally delete ric-8b in cardiac tissue in the adult animal after the addition of tamoxifen. Deletion of ric-8b led to severely reduced contractility as measured using echocardiography days after administration of tamoxifen. Histological analysis of the ventricular tissue showed highly variable myocyte size, prominent fibrosis and an increase in cellular apoptosis. At the cellular level, the deletion of ric-8b led to loss of activation of the L-type calcium channel through the β-adrenergic pathways. Using fluorescence resonance energy transfer based assays in heterologous expression systems we showed ric-8B protein selectively interacts with the stimulatory G-protein, Gαs. We then explored if deletion of gnas (the gene encoding Gαs) in cardiac tissue using a similar approach in the mouse led to an equivalent phenotype. The conditional deletion of the Gαs gene in the ventricle led to comparable effects on contractile function and cardiac histology. We conclude that ric-8b is essential to preserve cardiac contractile function likely through an interaction with the stimulatory G-protein. All mice were kept in a pathogen-free temperature-controlled environment (21-23°C) with 12-hour day/12-hour night light cycles. Animal were allowed access to standard rodent chow and water add-libitum. Mice were studied between 10-12 weeks of age. Use of animals in all the studies was in accordance with the United Kingdom Animal (Scientific Procedures) Act of 1986 and procedures were undertaken under PPL 70\7665 and PE9055EAD. Mice were killed by terminal anaesthesia.

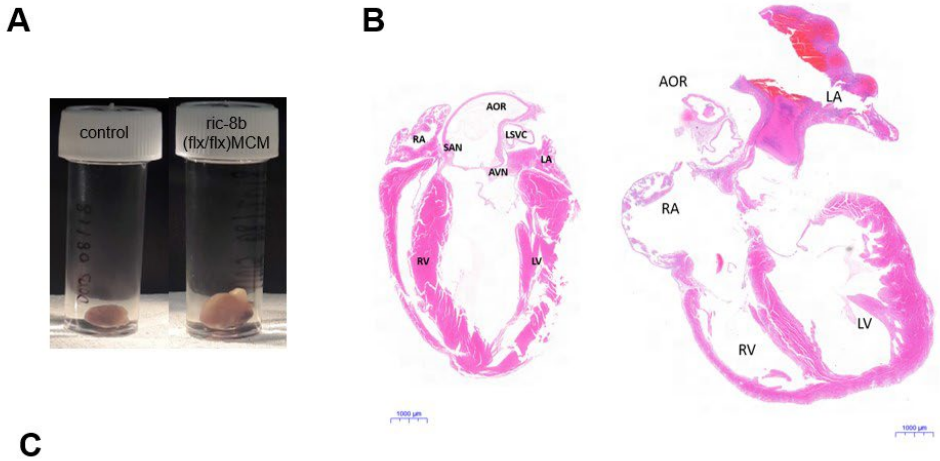

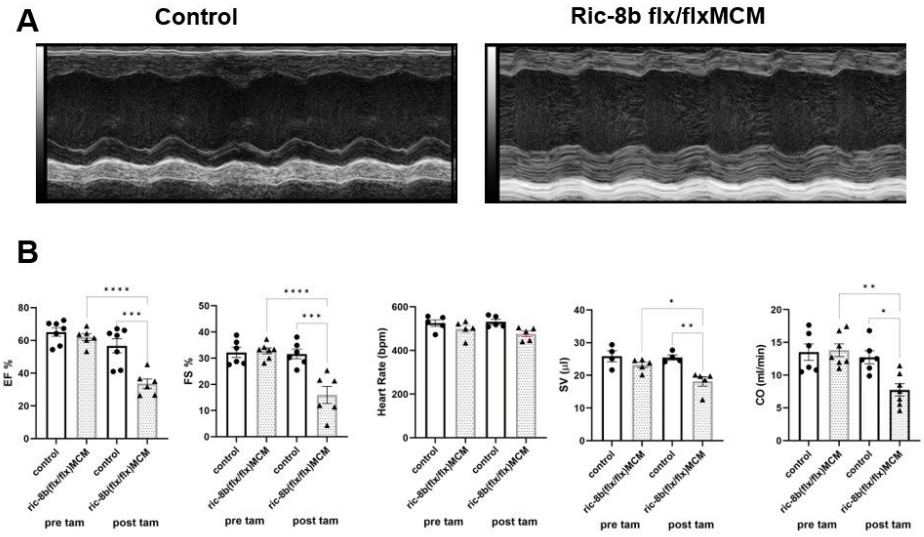

1. Nobles M, Benians A, Tinker A. Heterotrimeric G proteins precouple with G protein-coupled receptors in living cells. Proc Natl Acad Sci U S A 2005;102(51):18706-11. 2. Miller KG, Emerson MD, McManus JR, Rand JB. RIC-8 (Synembryn): a novel conserved protein that is required for G(q)alpha signaling in the C. elegans nervous system. Neuron 2000;27(2):289-299. 3. Tall GG, Krumins AM, Gilman AG. Mammalian Ric-8A (synembryn) is a heterotrimeric

Galpha protein guanine nucleotide exchange factor. J.Biol.Chem. 2003;278(10):8356-8362. 4. Kataria R, Xu X, Fusetti F, Keizer-Gunnink I, Jin T, Van Haastert PJ, Kortholt A. Dictyostelium Ric8 is a nonreceptor guanine exchange factor for heterotrimeric G proteins and is important for development and chemotaxis. Proc.Natl.Acad.Sci.U.S.A 2013;110(16):6424-6429. 5. Tall GG. Ric-8 regulation of heterotrimeric G proteins. J.Recept.Signal.Transduct.Res. 2013.

C30

The electrophysiological effect of antimalarial drug therapy

Shiraz Ahmad[1]

[1]University of Surrey, Guildford, United Kingdom, [2]University of Surrey, Guildford, United Kingdom

Antimalarial drug therapy is a cornerstone of the WHO strategy for malaria eradication. Antimalarial drug resistance is a problem in many parts of the world necessitating multi drug therapy. However since the early 1990s concerns have surrounded the cardiac electrophysiological effects of these drugs resulting in black box warnings for cardiac side effects. These have prevented mass drug administration and mass multi drug therapy in areas of malarial endemicity. However the underlying electrophysiological effect of these drugs if any has been poorly researched especially in combination. Here we use a loose patch clamp technique and intact right ventricular murine preparations to assess the effect if single and multidrug therapy on sodium and potassium channel function in an intact right ventricular preparation. We find significant reductions in sodium current with medloquine and chloroquine as well as indicators of am effect on potassium channel function with artemether/amodiaquine combination. Further data will confirm these effects and the effect on calcium homeostasis in the cell.